Applied Mathematical Modelling 44 (2017) 705–726

Contents lists available at ScienceDirect

Applied Mathematical Modelling

journal homepage: www.elsevier.com/locate/apm

Fractional-order exponential switching technique to enhance sliding mode control☆

Chun Yin [a,*], Xuegang Huang [b], Yangquan Chen [c], Sara Dadras [d], Shou-ming Zhong [e], Yuhua Cheng [a]

[a] School of Automation Engineering, University of Electronic Science and Technology of China, Chengdu 611731, PR China
[b] Hypervelocity Aerodynamics Institute, China Aerodynamics Research & Development Center, Mianyang 621000, PR China
[c] Mechatronics, Embedded Systems and Automation (MESA) Lab, School of Engineering, University of California, Merced, 5200 North Lake Road, Merced, CA 95343, USA
[d] Electrical and Computer Engineering Department, Utah State University, Logan, UT 84321, USA
[e] School of Mathematics Sciences, University of Electronic Science and Technology of China, Chengdu 611731, PR China

ARTICLE INFO

Article history:
Received 26 March 2015
Revised 18 January 2017
Accepted 14 February 2017
Available online 22 February 2017

Keywords:
Fractional-order
Sliding mode control
Switching technique
Reaching time
Stable region
Control performance

ABSTRACT

In this paper, a fractional-order sliding mode controller (FO SMC) based on an FO exponential switching technique and an FO proportional–integral (PI) switching surface is proposed for robust stabilization of uncertain FO nonlinear systems. The FO exponential switching technique, involving an FO sign function, is designed to guarantee the existence of the sliding motion in finite time. Reaching time is analytically derived and the reachability analysis is presented to explicate the superiority of the control performance. The stability analysis of sliding mode dynamics is performed relying on stable region analysis of FO systems. Simulation and practical results demonstrate the advantages of the designed control scheme.

© 2017 Elsevier Inc. All rights reserved.

1. Introduction

FO calculus [1–4] can date back to the end of the 17th century, when the classical IO calculus was established. In recent years, the applications of fractional order in science and engineering have attracted attention from researchers in different fields, such as developing FO control techniques. Providing more flexibility to enhance control performance, many FO controllers such as FO PID controllers and FO optimal controllers have aroused further interest [5–9]. For example, Yin et al. in [6] have shown the benefits of the FO extremum seeking control (ESC) over the IO ESC.

On the other hand, since that uncertainties and external disturbances always exist in many practical engineering plants, the robustness of the controllers is a necessary issue that must be concerned about in practical applications. Due to the strong robustness and attractiveness, the SMC has became a popular control technology and has been widely applied in science and engineering [10–16]. In [14], Feng et al. have discussed chattering free full-order sliding-mode control technique. In general, the design of SMC contains two phases: (a) definition of an appropriate sliding surface, (b) design of a control law to move the state variables to the surface. Recently, with the development of fractional calculus theory, the SMC has been

☆ This work was supported by National Basic Research Program of China (Grant 61503064 and 51502338) and 2015HH0039.
* Corresponding author.
E-mail addresses: yinchun.86416@163.com, chunyin@uestc.edu.cn (C. Yin).

http://dx.doi.org/10.1016/j.apm.2017.02.034
0307-904X/© 2017 Elsevier Inc. All rights reserved.

investigated for FO systems. Most published results about the FO SMC are restricted in FO linear systems under SMC [17], FO chaotic systems via SMC [18–21]. In [19], Yin et al. have studied the FO SMC for a general FO nonlinear system which can represent many FO chaotic system. Tavazoei et al. [18] have applied the SMC for the synchronization problem of the FO chaotic systems. Meanwhile, there are many application of FO SMC in practice [22], such as permanent magnet synchronous motor [23], antilock braking systems [24], electrostatic and electromechanical transducers[25] and wind turbines [26]. In [22], Zhong et al. have studied the application of the chattering-free variable structure control method based on fractional calculus. Zhang et al. [23] have investigated the FO SMC for the velocity control and the auto-tuning mechanism of parameters in the synchronous motor. Aghababa et al. in [25] have utilized the FO SMC to guarantee the stabilization of electrostatic and electromechanical transducers. The FO SMC has been considered as maximum power point tracking for wind turbines in [26]. Obviously, establishing direct systematic methods for proposing the FO SMC could be useful for some general FO nonlinear systems in engineering and scientific fields [27]. Hence, the investigation on direct systematic techniques is essential to guarantee desired robustness and performance criteria for general FO nonlinear systems, and the further analysis on how to improve control performance is needed for designing the FO SMC. Due to the absence of appropriate mathematical methods, most contributions about the FO SMC just focused on the FO equivalent control law to obtain the sliding surface, such as [17–27]. It should be mentioned that the switching law is another important part of SMC. The purpose of designing the switching law is to drive the plant's state trajectory to the desired sliding surface in finite time. Moreover, researchers want to further improve the convergence speed in reaching phase by investigating the switching technique and try to ensure that the chattering phenomenon won't be enlarged [28,29]. The shorten reaching time can guarantee that the system states could quickly approach to the sliding surface and become nonsensitive to the uncertainty and external disturbance. Chakrabarty et al. in [28] have investigated the generalized switching law for discrete time sliding mode control. Considering the better flexility of fractional calculus, the discussion and design for the FO switching technique could realize the above expectation. Although this scheme has been preliminarily discussed in our recent works [30,31], it also needs further exploration on the properties of the FO switching technique. Especially, it is necessary to analyze why and how to reduce reaching time and chattering as much as possible, when using the FO switching technique. Hence, in order to improve the control performance for general FO nonlinear systems, it is very important to investigate how to construct some direct systematic methods and FO switching techniques.

With this motivation, we propose an FO SMC with an FO switching technique and an FO PI sliding surface for uncertain FO nonlinear systems. For reachability analysis, an FO sign function $D_t^q \mathrm{sgn}(s), 0 \le q < 1,$ involving an FO differentiator, is introduced to construct the FO exponential rate switching law. $D_t^q \mathrm{sgn}(s)$ is proven to be able to ensure the reaching phase in finite time. The analytical reaching time t_{reach} under the FO exponential rate switching law is obtained, for the first time. The comparison of FO/IO exponential rate switching laws discloses the potential benefits of one controller over the other. For the stability analysis, the FO PI sliding surface is proposed for FO nonlinear systems. The stability condition of the FO sliding mode dynamics is discussed. The stable region analysis of FO systems is incorporated into the Lyapunov stability condition. Finally, simulation results show the advantages (i.e. faster and lower chattering performance) of the designed control scheme.

The rest of the paper is organized as follows: Section 2 shows problem formulation. Section 3 describes the sliding surface and controller design scheme. The reachability analysis is given in Section 4. The stability analysis is investigated in Section 5. In Section 6, simulation results are shown the effectiveness of the proposed controller. Finally, some concluding remarks are drawn in Section 7.

2. Problem statements

Consider the FO nonlinear system under uncertainty

$$\begin{aligned} \frac{d^{\beta}x(t)}{dt^{\beta}} &= (A+\delta(t))x(t)+Ff(x,t)+Bu(t), \\ y(t) &= \Psi x(t), \end{aligned} \tag{1}$$

where $x(t) \in R^n, u(t) \in R^n, y(t) \in R^{\upsilon}$ denote the state vector, input and output. $f(x, t) \in R^l$ is a nonlinear function. $A \in R^{n \times n}$, $F \in R^{n\times l}, B \in R^{n\times n}, \Psi \in R^{\upsilon\times n}$ are constant known matrices. Furthermore, B is reversible. The fractional order β satisfies $0 < \beta < 1$. The uncertainty $\delta(t) = WG(t)N,$ in which W, N are known real constant matrices, $\|G(t)\| < 1$, $\forall t > 0$. To derive main results, the following definition and lemmas are used.

Definition 2.1. [1] The fractional integral with $\alpha \in (0, 1)$ is defined as follows:

$$I_t^{\alpha}\zeta(t) = \frac{1}{\Gamma(\alpha)}\int_0^t (t-\tau)^{\alpha-1}\zeta(\tau)d\tau, \tag{2}$$

in which $\zeta(t)$ denotes any properly behaved function, Γ is the Gamma function. The Riemann–Liouville definition of the $\bar{\beta}$th-order derivative is

$$\frac{d^{\bar{\beta}}\zeta(t)}{dt^{\bar{\beta}}} = \frac{1}{\Gamma(n-\bar{\beta})}\left(\frac{d}{dt}\right)^n \int_0^t \frac{\zeta(\tau)}{(t-\tau)^{1+\bar{\beta}-n}}d\tau, \tag{3}$$

in which $n-1 \le \bar{\beta} < n$, n is an integer.

Lemma 2.1. *[8] For* $D_t^{\tilde{\beta}}\sigma(t)=\frac{1}{\Gamma(1-\tilde{\beta})}\frac{d}{dt}\int_0^t\frac{\sigma(\tau)}{(t-\tau)^{\tilde{\beta}}}d\tau$ *with* $\sigma(t)\in R, 0\le\tilde{\beta}<1$ *and the sign function, one has*

$$D_t^{\tilde{\beta}}\mathrm{sgn}(\sigma(t))\begin{cases}>0, & \text{if}\quad \sigma(t)>0, t>0,\\ <0, & \text{if}\quad \sigma(t)<0, t>0.\end{cases} \tag{4}$$

Remark 2.1. A concept of the FO sign function $D_t^{\tilde{\beta}}\mathrm{sgn}(\sigma)$, including an FO differentiator, has been firstly proposed to extract the sign of σ in our recent work [8]. Similar to the sign function, $D_t^{\tilde{\beta}}\mathrm{sgn}(\sigma)$ is demonstrated to be capable of extracting the sign of σ. One may think it is trivial compared with the sign function itself; others may doubt that it is against instinct compared with the derivative of a generic function. The meaning of $D_t^{\tilde{\beta}}\mathrm{sgn}(\sigma), 0\le\tilde{\beta}<1$ is the **fractional order derivative** of the sign function. The derivative represents a measure of how a function changes as its input changes. The sign of the derivative is generally not the same as the sign of the function itself. However, the sign of the FO sign function $D_t^{\tilde{\beta}}\mathrm{sgn}(\sigma), 0\le\tilde{\beta}<1$ is proven to be the same as the sign function $\mathrm{sgn}(\sigma)$ in our recent work [8]. This is an important property of the FO sign function.

Remark 2.2. The FO sign function will be applied to build an FO switching function. According to Lemma 2.1, the corresponding FO switching function can guarantee to force the system on the sliding surface. It will be shown in the following.

Lemma 2.2. *[32] The autonomous system* $D_t^{\rho}\varsigma=\bar{A}\varsigma, \varsigma(0)=\varsigma_0$, *in which* ρ *denotes the differential order,* $\varsigma\in R^n$ *and* $\bar{A}\in R^{n\times n}$, *is asymptotically stable if* $|\arg(eig(\bar{A}))|>\rho\pi/2$. *Furthermore, the system is stable if* $|\arg(eig(\bar{A}))|\ge\rho\pi/2$ *and those critical eigenvalues that satisfy* $|\arg(eig(\bar{A}))|=\rho\pi/2$ *have geometric multiplicity one.*

Lemma 2.3. *[32] For any matrix* M_1 *and* M_2 *of compatible dimensions and any scalar* $\zeta>0$, *one has* $M_1^TM_2+M_2^TM_1\le\zeta M_1^TM_1+(1/\zeta)M_2^TM_2$.

Lemma 2.4. *[33] For constant matrices* Π_1, Π_2, Π_3, *in which* $\Pi_1=\Pi_1^T$, *and* $\Pi_2=\Pi_2^T>0$, *then* $\Pi_1+\Pi_3^T\Pi_2^{-1}\Pi_3<0$ *if and only if*

$$\begin{bmatrix}\Pi_1 & \Pi_3^T\\ \Pi_3 & -\Pi_2\end{bmatrix}<0,\quad\text{or}\quad\begin{bmatrix}-\Pi_2 & \Pi_3\\ \Pi_3^T & \Pi_1\end{bmatrix}<0. \tag{5}$$

3. Sliding surface and control scheme design

Firstly, the sliding surface is selected as

$$s=C_1D_t^{\beta-1}x+C_2z, \tag{6}$$

in which $\dot{z}=\bar{K}x-D_t^{1-\beta}z$, with $s=[s_1,s_2,\dots,s_n]^T\in R^n, z\in R^{\iota}, C_1\in R^{n\times n}, C_2\in R^{n\times\iota}, \bar{K}\in R^{\iota\times n}$. Furthermore, C_1 is reversible. Define $\mathrm{sgn}(s):R^n\to R^n, D_t^q\mathrm{sgn}(s):R^n\to R^n$ as follows:

$$\begin{aligned}\mathrm{sgn}(s)&=[\mathrm{sgn}(s_1),\mathrm{sgn}(s_2),\dots,\mathrm{sgn}(s_n)]^T,\\ D_t^q\mathrm{sgn}(s)&=[D_t^{q_1}\mathrm{sgn}(s_1),D_t^{q_2}\mathrm{sgn}(s_2),\dots,D_t^{q_n}\mathrm{sgn}(s_n)]^T,\end{aligned}$$

with $0\le q_i<1, (i=1,2,\dots,n)$. Then, an FO exponential rate switching law is defined as:

$$\begin{aligned}u_{sw}&=-HD_t^q\mathrm{sgn}(s(t))-Ks(t)\\ &=-\begin{bmatrix}h_1&0&\cdots&0\\0&h_2&\cdots&0\\ \vdots&\vdots&\ddots&\vdots\\0&0&\cdots&h_n\end{bmatrix}\begin{bmatrix}D_t^{q_1}\mathrm{sgn}(s_1)\\D_t^{q_2}\mathrm{sgn}(s_2)\\ \vdots\\D_t^{q_n}\mathrm{sgn}(s_n)\end{bmatrix}-\begin{bmatrix}k_1&0&\cdots&0\\0&k_2&\cdots&0\\ \vdots&\vdots&\ddots&\vdots\\0&0&\cdots&k_n\end{bmatrix}\begin{bmatrix}s_1\\s_2\\ \vdots\\s_n\end{bmatrix},\end{aligned} \tag{7}$$

where $H=\mathrm{diag}(h_1,h_2,\dots,h_n), K=\mathrm{diag}(k_1,k_2,\dots,k_n)$ with $h_i,k_i>0, (i=1,2,\dots,n)$.

Remark 3.1. The FO sign functions $D_t^{q_i}\mathrm{sgn}(s_i), q_i\in[0,1), i=1,2,\dots,n$ are applied to built the FO exponential rate switching law. Note that $\mathrm{sgn}(s_i)$ (i.e. $q_i=0$) is a special case of $D_t^{q_i}\mathrm{sgn}(s_i)$. Therefore, the classical IO exponential rate switching law is equivalent to the above FO exponential rate switching law with $q_i=0$. Hence, there is a better flexibility in adjusting FO than IO exponential rate switching law.

Based on (6) and (7), a SMC is given by

$$u=-(C_1B)^{-1}[(C_1A+C_2\bar{K}+C_1)x+C_1Ff(x,t)+\bar{u}], \tag{8}$$

in which $\bar{u}=w_1+Ks-D_t^{1-\beta}s$ with $w_1=\|C_1W\|\|Nx\|\mathrm{sgn}(s)+HD_t^q\mathrm{sgn}(s)$. Fig. 1 shows the block diagram of the proposed control strategy.

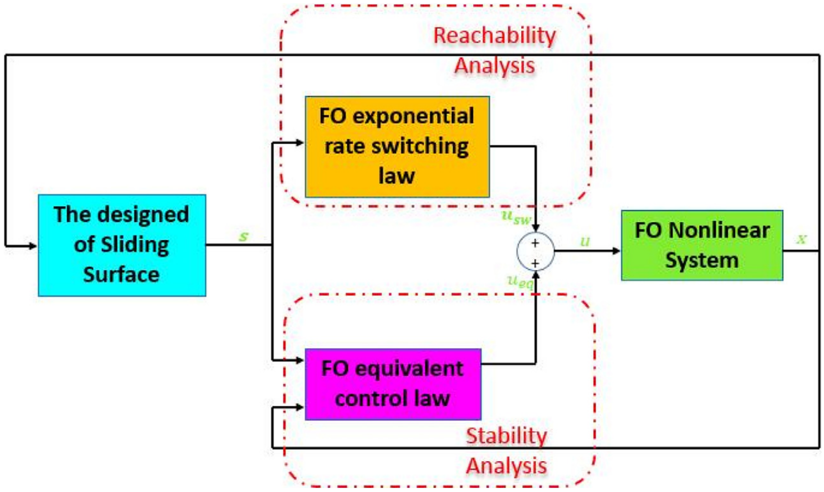

Fig. 1. The block diagram of the control strategy.

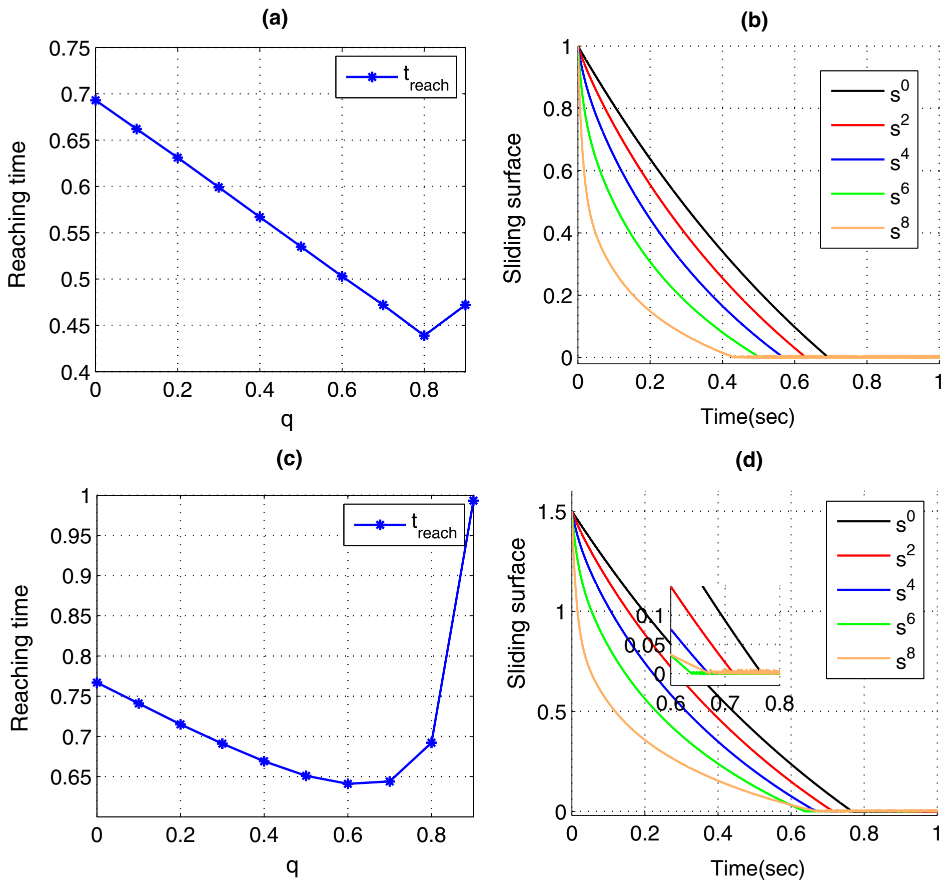

Fig. 2. (a) The solutions t_{reach} of $\int_0^{t_{reach}} \tau^{-q} e^{\tau} d\tau = \Gamma(1-q)$ when $q = 0, 0.1, \ldots, 0.9$, respectively. (b) The solutions s^j of $\dot{s}^j = -s^j - D_t^{q^j}(\text{sgn}(s^j))$, $(j = 0, 2, 4, 6, 8)$ with $q^0 = 0, q^2 = 0.2, q^4 = 0.4, q^6 = 0.6, q^8 = 0.8$, when $s^j(0) = 1$. (c) The solutions t_{reach} of $\int_0^{t_{reach}} \tau^{-q} e^{k\tau} d\tau = \frac{1.5\Gamma(1-q)}{1.3}$, where $q = 0, 0.1, \ldots, 0.9$, respectively. (d) The solutions s^j of $\dot{s}^j = -s^j - 1.3D_t^{q^j}(\text{sgn}(s^j))$ with $q^0 = 0, q^2 = 0.2, q^4 = 0.4, q^6 = 0.6, q^8 = 0.8$, when $s^j(0) = 1.5$**.**

Remark 3.2. The FO exponential rate switching law $u_{sw}(t)$ is firstly introduced in the manuscript. Comparing with the traditional IO switching law $u_{IO-sw} = -K_c \text{sgn}(s(t)), K_c = \text{diag}(k_{c1}, \ldots, k_{cn})$ with $k_{ci} > 0, (i = 1, \ldots, n)$ adopted in [13–16,19–21,23,26,27], $u_{sw}(t)$ contains the proportional rate term $-HD_t^q \text{sgn}(s(t))$ and the FO sign function $D_t^{q_i} \text{sgn}(s_i), q_i \in [0, 1), i = 1, 2, \ldots, n$. The terms $-HD_t^q \text{sgn}(s(t))$ could push the state to converge to the switching manifold faster when $s(t)$ is large.

Table 1
Calculation formulae of reaching time.

Switching law	Reaching time t_{reach} $(s \in R)$	Reaching time t_{reach} $(s \in R^n)$
IO version	$\frac{1}{k}\ln\frac{h+k\lvert s(0)\rvert}{h}$	$\max\left\{\frac{1}{k_i}\ln\frac{h_i+k_i\lvert s_i(0)\rvert}{h_i}, i=1,\ldots,n\right\}$
FO version	$\int_0^{t_{reach}}\tau^{-q}e^{k\tau}d\tau=\frac{\lvert s(0)\rvert\Gamma(1-q)}{h}$ *	$\max\left\{\int_0^{t^i_{reach}}\tau^{-q_i}e^{k_i\tau}d\tau=\frac{\lvert s_i(0)\rvert\Gamma(1-q_i)}{h_i}*, i=1,\ldots,n\right\}$

* t_{reach} under the FO exponential rate switching law can be obtained from this equation by applying the intermediate value theorem.

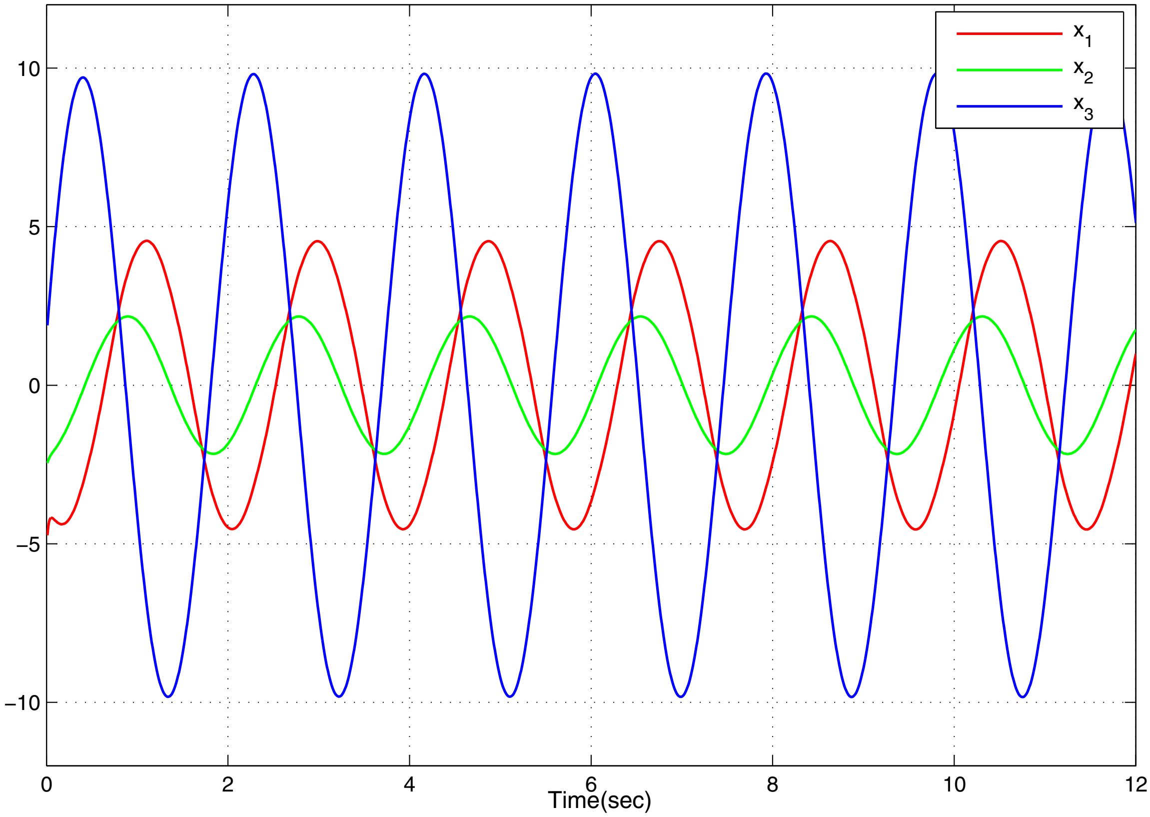

Fig. 3. Time responses of the FO n-scroll attractor (26) without the controller and the uncertainty.

Moreover, for $|D_t^{q_i}\mathrm{sgn}(s_i)|$, it is more likely to choose a series of $q_i \in [0, 1)$ such that $|D_t^{q_i}\mathrm{sgn}(s_i)|$ is bigger than 1 during the initial time interval, and $|D_t^{q_i}\mathrm{sgn}(s_i)| \le 1$ during the next time interval, as analyzed in [6]. So, the proposed FO switching type control law $u_{sw}(t)$ could increase the reaching speed when the state is far away from the switching manifold. Furthermore, it reduces the rate when the state is near the switching manifold. The result can be expected to be fast with a low chattering reaching mode. For the traditional IO switching control law u_{IO-sw}, it constrains the state to reach $s(t)$ at a constant rate K_c. If K_c is too small, the reaching time will be too long. Otherwise, a very large K_c will result in high chattering. Hence, u_{IO-sw} cannot improve the control performance by reducing reaching time and chattering simultaneously, while, the the control structure of $u_{sw}(t)$ could be expected to improve the control performance of sliding mode method.

4. Reachability analysis

The reachability analysis will be considered.

Theorem 4.1. *Consider the FO system (1), the state trajectories under the controller (8) with the FO exponential rate switching law (7) can achieve $s(t) = 0$ in finite time.*

Proof. Considering $V(t) = s^T(t)s(t)$, one has

$$\dot{V} = [C_1\delta(t)x - w_1 - Ks]^T s + s^T[C_1\delta(t)x - w_1 - Ks].$$

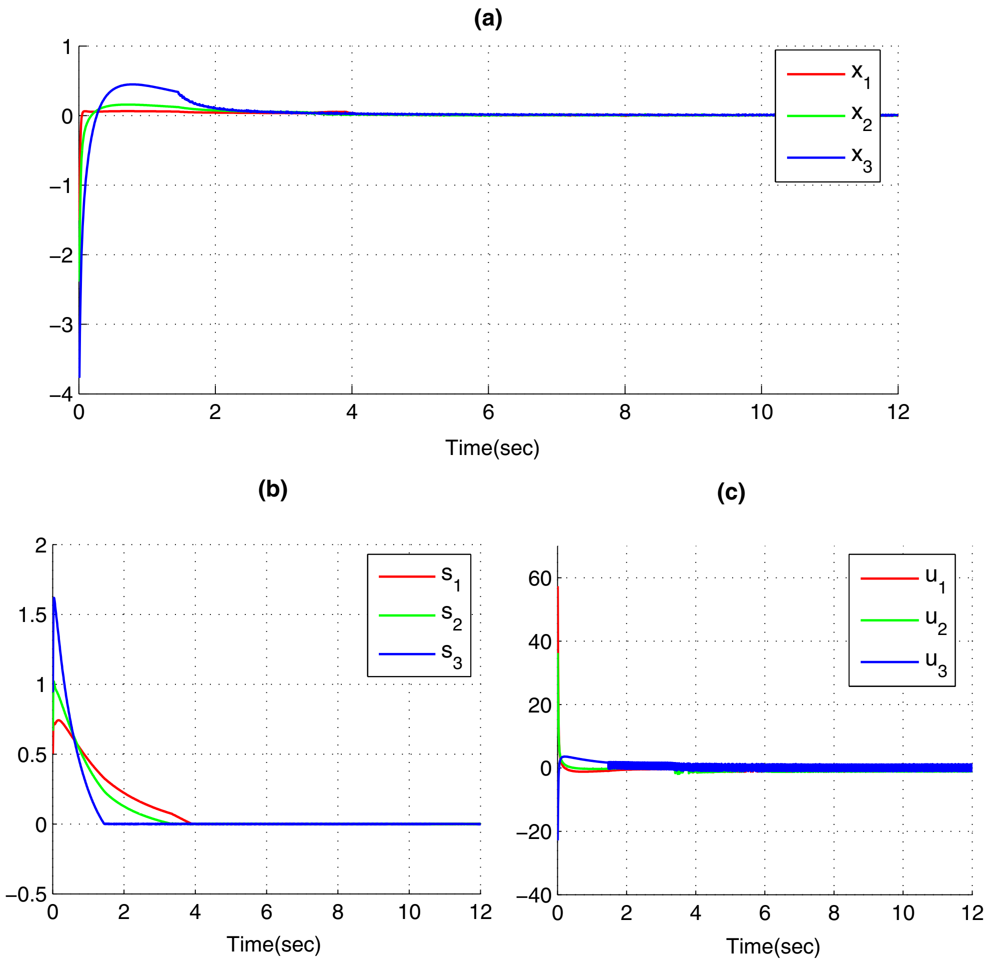

Fig. 4. Time responses of the FO n-scroll attractor (26) under the controller (28); (b) the time response of the sliding surface (29); (c) the time response of the FO SMC (28).

Since $\|G(t)\| < 1$, one has

$$\begin{aligned}\dot{V} &\le \Omega + \Omega^T - (s^T H D_t^q \mathrm{sgn}(s) + (H D_t^q \mathrm{sgn}(s))^T s + 2s^T K s)\\ &\le -(s^T H D_t^q \mathrm{sgn}(s) + (H D_t^q \mathrm{sgn}(s))^T s + 2s^T K s),\end{aligned} \tag{9}$$

where $\Omega = s^T C_1 \delta(t) x - s^T \|C_1 W\| \|Nx\| \mathrm{sgn}(s)$. From Lemma 2.1, one has $\dot{V} < 0$. Thus, the controlled system can reach the switching surface in finite time. The proof is completed. □

Next, the **calculation formula** of **reaching time** will be discussed and computed.

First, we consider $s(t) \in R$. Then, we have $0.5\dot{V} = s\dot{s} \le -hsD_t^q \mathrm{sgn}(s) - ks^2 \le 0$, in which $0 \le q < 1$ and h, k are positive constants. Let $s\dot{s} = -hsD_t^q \mathrm{sgn}(s) - ks^2 \le 0$.

Before deriving t_{reach} under the FO exponential rate switching law, t_{reach} under the IO exponential rate switching law $u_{sw} = -h\mathrm{sgn}(s) - ks$ will be calculated. For the IO exponential rate switching law, one has $s\dot{s} = -h|s| - ks^2 \le 0$. There are two cases: **1)** When $s(0) > 0$, one has

$$\dot{s}(t) = -ks - h \Rightarrow \dot{s}(t) + ks = -h. \tag{10}$$

Since $(s(t)e^{kt})' = e^{kt}(\dot{s}(t) + ks) = -he^{kt}$, one obtains $s(t)e^{kt} - s(0) = \frac{h}{k} - \frac{h}{k}e^{kt}$.

Thus, one can conclude $s(t) = (s(0) + \frac{h}{k})e^{-kt} - \frac{h}{k}$. Since $s(t_{reach}) = 0$, one has

$$t_{reach} = \frac{1}{k} \ln \frac{s(0) + \frac{h}{k}}{\frac{h}{k}} = \frac{1}{k} \ln \frac{ks(0) + h}{h} > 0. \tag{11}$$

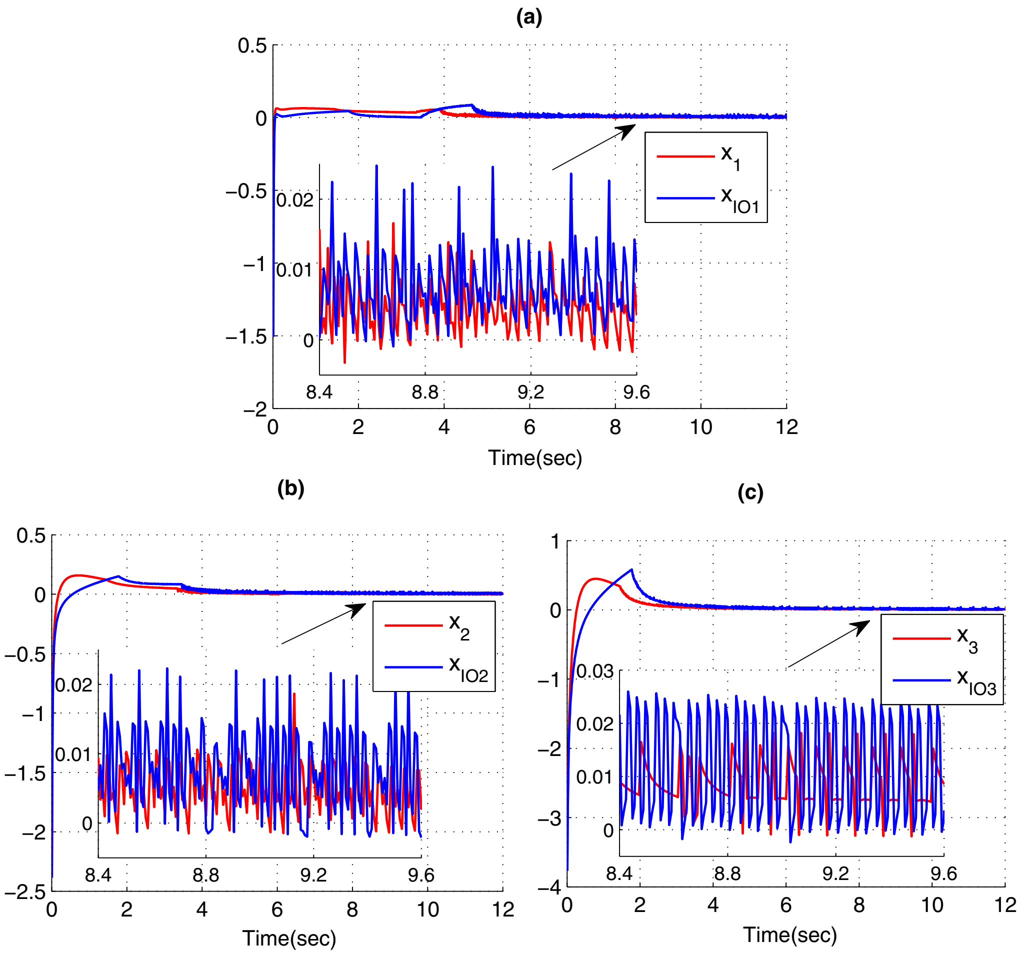

Fig. 5. Time responses of the states x_1, x_2, x_3 under the proposed controller (28), the states x_{IO1}, x_{IO2}, x_{IO3} under u_{IO}.

2) When $s(0) < 0$, one has $\dot{s}(t)=-ks+h \Rightarrow \dot{s}(t)+ks=h$. Similarly, one has $s(t)e^{kt}-s(0)=\frac{h}{k}e^{kt}-\frac{h}{k}$. Hence, it can be obtained that $s(t) = (s(0)-\frac{h}{k})e^{-kt}+\frac{h}{k}$. At $t=t_{reach}$, $s(t_{reach})=0$. Thus,

$$t_{reach} = \frac{1}{k}\ln\frac{\frac{h}{k}-s(0)}{\frac{h}{k}} = \frac{1}{k}\ln\frac{h-ks(0)}{h} > 0. \tag{12}$$

According to the above analysis from cases **1)-2)**, one can obtain t_{reach} under the IO exponential rate switching law as follows

$$t_{reach} = \frac{1}{k}\ln\frac{h+k|s(0)|}{h} > 0. \tag{13}$$

Similarly, t_{reach} under the FO exponential rate switching law will be calculated as follows:

3) When $s(0) > 0$, one has $\dot{s}(t)=-ks-hD_t^q\mathrm{sgn}(s)$ where $D_t^q\mathrm{sgn}(s)=\frac{1}{\Gamma(1-q)}\frac{d}{dt}\int_0^t\frac{\mathrm{sgn}(s(\tau))}{(t-\tau)^q}d\tau$. Hence, one has $\dot{s}(t)=-ks(t)-\frac{h}{\Gamma(1-q)}\frac{d}{dt}\int_0^t\frac{1}{(t-\tau)^q}d\tau$. Furthermore, one has

$$\left(s(t)e^{kt}\right)' = e^{kt}(\dot{s}(t)+ks) = -\frac{he^{kt}}{\Gamma(1-q)}\frac{d}{dt}\int_0^t\frac{1}{(t-\tau)^q}d\tau. \tag{14}$$

Hence, $s(t)e^{kt}=s(0)-\frac{h}{\Gamma(1-q)}\int_0^t\tau^{-q}e^{k\tau}d\tau$. Due to $s(t_{reach})=0$, one has $s(t_{reach})e^{kt_{reach}}=s(0)-\frac{h}{\Gamma(1-q)}\int_0^{t_{reach}}\tau^{-q}e^{k\tau}d\tau=0$.

So, the solution of $s(0)=\frac{h}{\Gamma(1-q)}\int_0^t\tau^{-q}e^{k\tau}d\tau$ is t_{reach}. Let $\vartheta(t)=\int_0^t\tau^{-q}e^{k\tau}d\tau=\frac{s(0)\Gamma(1-q)}{h}>0$. Obviously, $\vartheta(t)$, $t\in[0,\infty)$ is an increasing function, $\vartheta(0)=0$ and $\vartheta(\infty)=\infty$. Based on the intermediate value theorem, there exists $t^*>0$ such that $\vartheta(t^*)=\int_0^{t^*}\tau^{-q}e^{k\tau}d\tau=\frac{s(0)\Gamma(1-q)}{h}$. Hence, we can use numerical approximation to obtain $t_{reach}=t^*$.

4) When $s(0)<0$, one has $\dot{s}(t)=-ks-hD_t^q\mathrm{sgn}(s)$. Hence, one has $\dot{s}(t)=-ks(t)-\frac{h}{\Gamma(1-q)}\frac{d}{dt}\int_0^t\frac{-1}{(t-\tau)^q}d\tau$. Similar to **3)**, $(s(t)e^{kt})'=e^{kt}(\dot{s}(t)+ks)=\frac{he^{kt}}{\Gamma(1-q)}\frac{d}{dt}\int_0^t\frac{1}{(t-\tau)^q}d\tau$. One has $s(t_{reach})e^{kt_{reach}}=s(0)+\frac{h}{\Gamma(1-q)}\int_0^{t_{reach}}\tau^{-q}e^{k\tau}d\tau=0$.

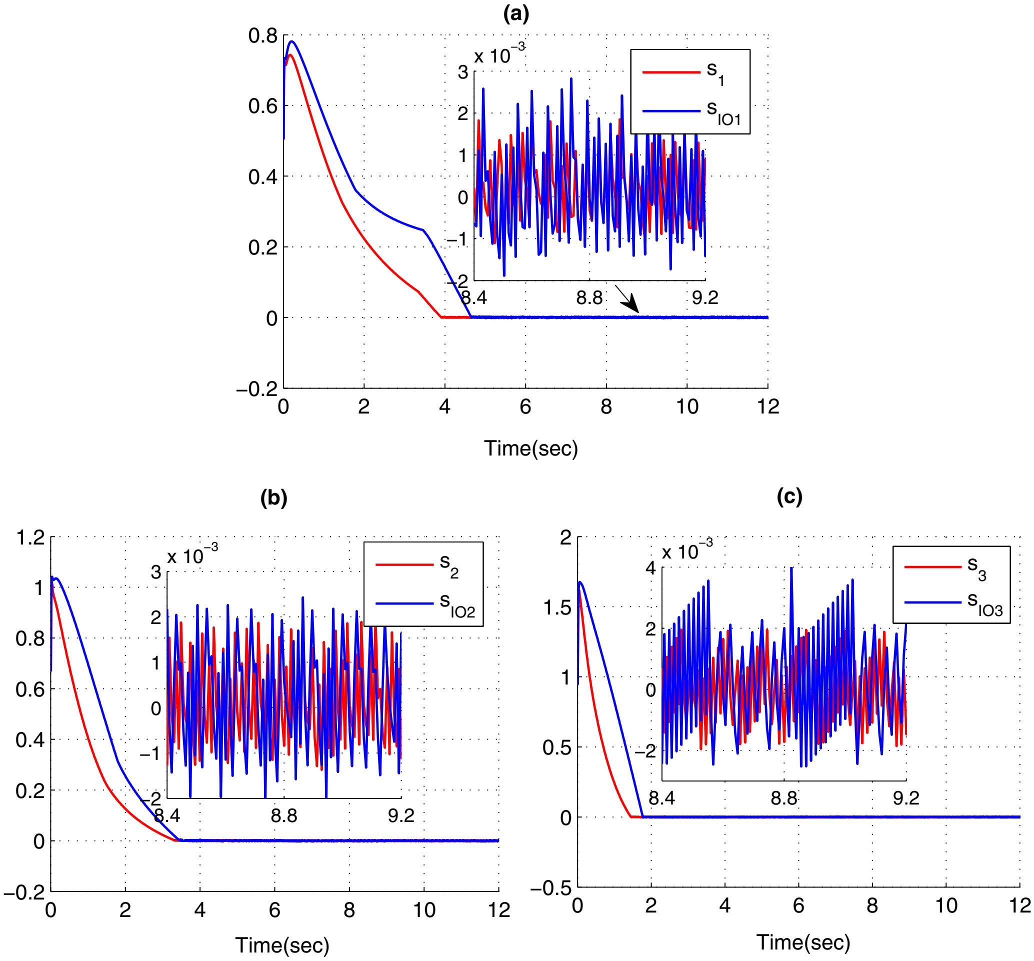

Fig. 6. Time responses of the sliding functions s_1, s_2, s_3 (29) under the proposed controller (28), s_{IO1}, s_{IO2}, s_{IO3} under u_{IO}.

Let $\vartheta(t)=\int_0^t \tau^{-q}e^{k\tau}d\tau=\frac{s(0)\Gamma(1-q)}{-h}>0$. Since $\vartheta(t)$, $t\in[0,\infty)$ is an increasing function, $\vartheta(0)=0$ and $\vartheta(\infty)=\infty$. Based on the intermediate value theorem again, there exists $t^*>0$ such that $\vartheta(t^*)=\frac{-s(0)\Gamma(1-q)}{h}$. So, the reaching time $t_{reach}=t^*$ can be found by numerical approximation.

From the analysis in cases **3)**-**4)**, t_{reach} of the FO exponential rate switching law can be obtained from $\vartheta(t)=\int_0^t \tau^{-q}e^{k\tau}d\tau=\frac{|s(0)|\Gamma(1-q)}{h}$.

Remark 4.1. From the **calculation formulae**, the parameters $s(0)$, h, k and q have impact on t_{reach}. For $s(t)\in R$, the above analysis can also be used to derive a shorter t_{reach} by adjusting q, such as the following cases (**I**-**II**). Let $k=1$.

(I) When $|s(0)|=h=1$, the solutions t_{reach} of $\int_0^{t_{reach}} \tau^{-q}e^{k\tau}d\tau=\frac{|s(0)|\Gamma(1-q)}{h}$ are depicted in Part (a) of Fig. 2, where $q=0,0.1,\ldots,0.9$, respectively. It can be seen that t_{reach} under $q=0.8$ is the smallest in this case.

Meanwhile, the solutions of $\dot{s}^j=-s^j-D_t^{q^j}(\text{sgn}(s^j))$ are shown in Part (b) of Fig. 2, in which $s(0)=1$ and $q^0=0, q^2=0.2, q^4=0.4, q^6=0.6, q^8=0.8$, respectively. It shows that t_{reach} of s^8 is the shortest. Furthermore, the reaching times of s^j, $j=0,2,4,6,8$ in Part (b) are the same as t_{reach} in Part (a) of Fig. 2.

(II) When $|s(0)|=1.5$ and $h=1.3$, Part (e) of Fig. 2 shows the solutions t_{reach} of $\int_0^{t_{reach}} \tau^{-q}e^{k\tau}d\tau=\frac{|s(0)|\Gamma(1-q)}{h}$, where $q=0,0.1,\ldots,0.9$. It shows that t_{reach} under $q=0.6$ is the smallest in this case. The solutions s^j of $\dot{s}^j=-s^j-1.3D_t^{q^j}\text{sgn}(s^j)$ are depicted in Part (f) of Fig. 2, when $s(0)=1.5$ and $q^0=0, q^2=0.2, q^4=0.4, q^6=0.6, q^8=0.8$. It can verify the accuracy of the above result.

Next, for $s=[s_1(t),s_2(t),\ldots,s_n(t)]^T\in R^n$, t^i_{reach} of $s_i(t)$, $(i=1,2,\ldots,n)$ under the FO exponential rate switching law can be obtained from this equation

$$\int_0^{t^i_{reach}} \tau^{-q_i}e^{k_i\tau}d\tau=\frac{|s_i(0)|\Gamma(1-q_i)}{h_i} \tag{15}$$

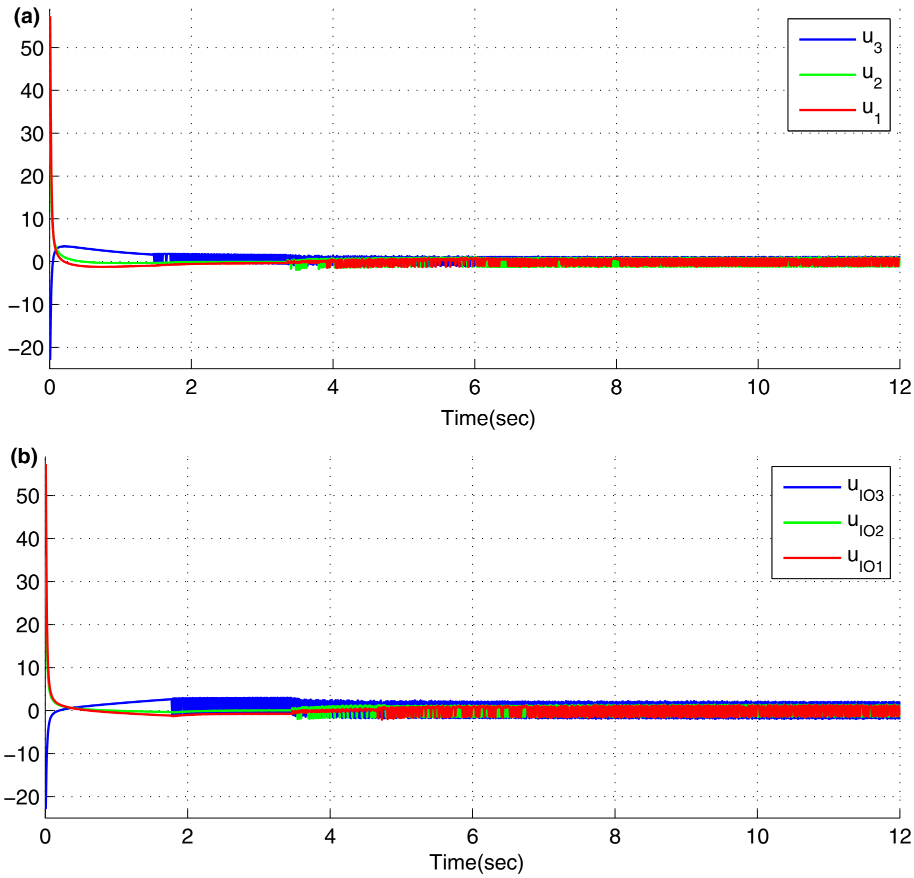

Fig. 7. Time responses of u and u_{IO}.

by using numerical approximation, as same as the analysis in **3)**-**4)**. Hence, one obtains $t_{reach} = \max\{t^i_{reach}, i = 1, 2, \dots, n\}$. The **calculation formulae** of t_{reach} under the FO and IO exponential rate switching law are listed in Table 1.

Remark 4.2. Clearly, $\mathrm{sgn}(s)$ is a special case of $D^q_t(\mathrm{sgn}(s)), 0 \le q_i < 1, (i = 1, \dots, n)$, since

$$D^0_t \mathrm{sgn}(s_i(t)) = \frac{1}{\Gamma(1-0)} \frac{d}{dt} \int_0^t \frac{\mathrm{sgn}(s_i(\epsilon))}{(t-\epsilon)^0} d\epsilon = \mathrm{sgn}(s_i(t)), \quad , i = 1, 2, \dots, n.$$

Hence, u_{sw} with $D^q_t(\mathrm{sgn}(s)), 0 \le q_i < 1$ can be considered as an FO/IO controller synthesis (*i.e. IO law* $-H\mathrm{sgn}(s) - Ks$ *with* $\mathrm{sgn}(s)$ *and FO law* $-HD^q_t \mathrm{sgn}(s) - Ks$, *with* $D^{q_i}_t \mathrm{sgn}(s_i(t)), 0 < q_i < 1, (i = 1, 2, \dots, n)$). In the other words, the IO law $-H\mathrm{sgn}(s) - Ks$ is equal to the above FO exponential rate switching law $\mathrm{sgn}(s)$ and FO law $-HD^q_t \mathrm{sgn}(s) - Ks$ when $q_i = 0, (i = 1, 2, \dots, n)$. Therefore, the overall FO exponential rate switching law with $D^{\bar{\beta}}(\mathrm{sgn}(s(t))), 0 \le \bar{\beta} < 1$ could be expected to improve the system performance, when just considering $-H\mathrm{sgn}(s) - Ks$ applied in [17,18,22,24,25]. Nonetheless, choosing $q_i = 0, (i = 1, 2, \dots, n)$ for some special systems could result in a better performance. However, there would be no contradiction, since the switching type control law $-H\mathrm{sgn}(s) - Ks$ is the special case of the proposed FO exponential rate switching law $-HD^q_t \mathrm{sgn}(s) - Ks, 0 < q_i < 1, (i = 1, 2, \dots, n)$. The following simulations results will show the potential advantage of the proposed method.

Remark 4.3. From the equivalent control concept, SMC has this form $u = u_{eq} + u_{sw}$, in which u_{eq} and u_{sw} represent the equivalent control law and the switching law, respectively. In this paper, the FO sliding surface is considered to develop direct systematic methods for designing SMC for FO nonlinear systems. The FO exponential rate switching law based on $D^q_t \mathrm{sgn}(s)$ is proposed and the corresponding calculation formulae in Table 1 is deduced by utilizing the property of $D^q_t \mathrm{sgn}(s)$. From the property of $D^q_t \mathrm{sgn}(s)$ and the calculation formulae in Table 1, a shorter reaching time can be derived by choosing the parameters q_i, h_i, k_i, $s_i(0)$. Although the choice of q_i, h_i, k_i, $s_i(0)$ has the influence on the control performance, it is a bit difficult to analyze how q_i affects the control performance (i.e. reaching time and chattering) when comparing the other parameters h_i, k_i, $s_i(0)$. However, the calculation formulae in Table 1 of the manuscript could be helpful to built a tuning mechanism for the controller parameters including q_i. Our technique are suitable for solving this issue and this is a topic of our future research.

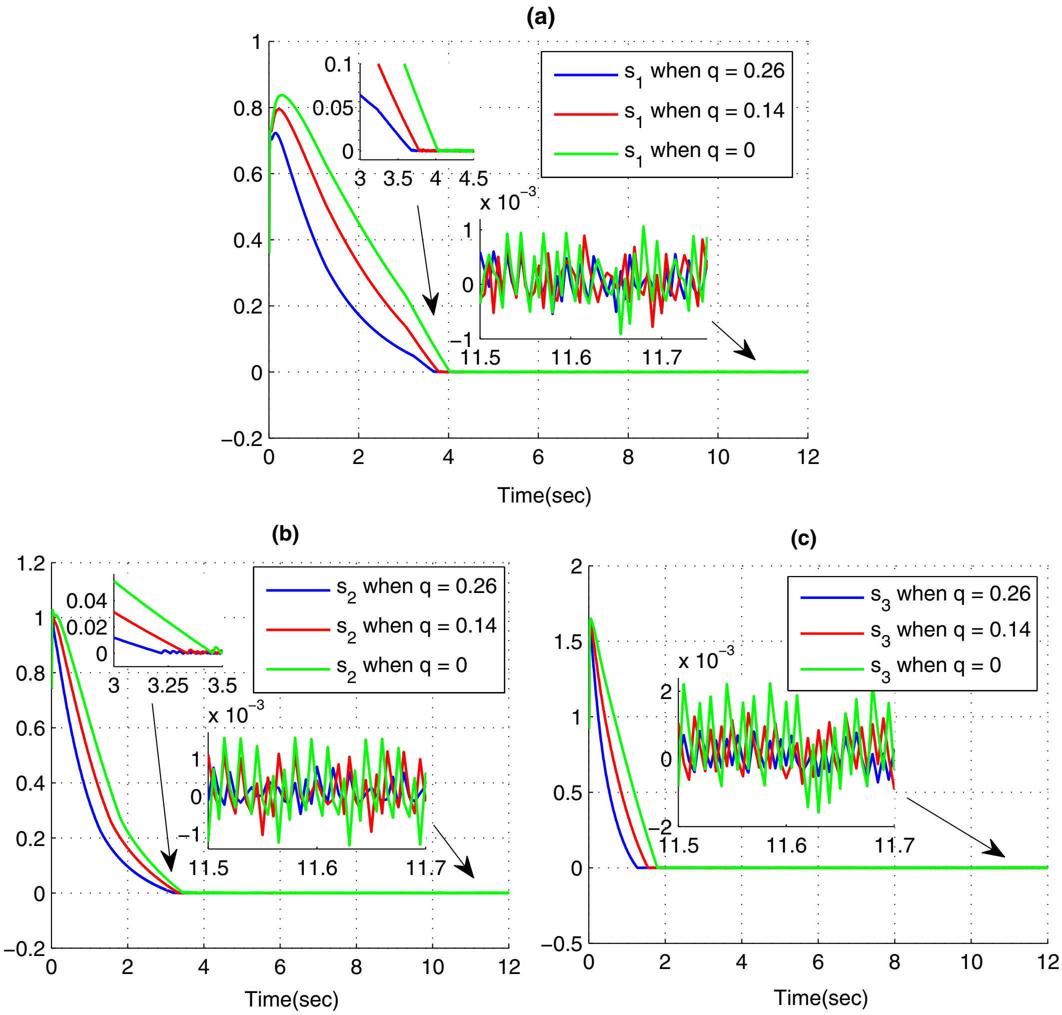

Fig. 8. Time responses of the sliding functions s_1, s_2, s_3 under the proposed FO exponential rate switching law $u_{sw} = -HD_t^q \text{sgn}(s) - Ks$ with $q = 0.26, 0.14, 0$.

5. Stability analysis

Next, the stability analysis of the sliding mode dynamics will be investigated. First, the following proposition is given.

Proposition 5.1. *The FO system $D_t^\beta \varsigma = \bar{A}\varsigma, \varsigma(0) = \varsigma_0, 0 < \beta < 1$ is asymptotically stable if the IO system $D\varsigma = \bar{A}\varsigma, \varsigma(0) = \varsigma_0$ is asymptotically stable.*

Proof. For the IO systems $D\varsigma = \bar{A}\varsigma$, it is well-known that the stability condition of the IO systems is

$$\text{Re}(\lambda_j(\bar{A})) < 0, j = 1, 2, \ldots, n, \tag{16}$$

where $\lambda_j(\bar{A})$ is the jth eigenvalue of A. Furthermore, the above condition is equivalent to the following:

$$|\arg(\lambda_j(\bar{A}))| > \pi/2, j = 1, 2, \ldots, n, \tag{17}$$

where arg represents the argument of $\lambda_j(\bar{A})$. In other words, the stability condition can be concluded that

$$\begin{aligned} |sI - \bar{A}| &= (s - \lambda_1(\bar{A}))(s - \lambda_2(\bar{A})) \cdots (s - \lambda_n(\bar{A})) = 0 \\ &\Longrightarrow \text{Re}(\lambda_j(\bar{A})) < 0, j = 1, 2, \ldots, n. \end{aligned} \tag{18}$$

$$\begin{aligned} &\text{Since} \quad \lambda_j(\bar{A}) = r_j(\cos\phi_j + i\sin\phi_j) = r_j e^{i\phi_j} \quad \text{where} \quad r_j = |\lambda_j(\bar{A})|, \phi_j = \arg(\lambda_j(\bar{A}))), \\ &\qquad \Longrightarrow |\phi_j| = |\arg(\lambda_j(\bar{A}))| > \pi/2, j = 1, 2, \ldots, n. \end{aligned} \tag{19}$$

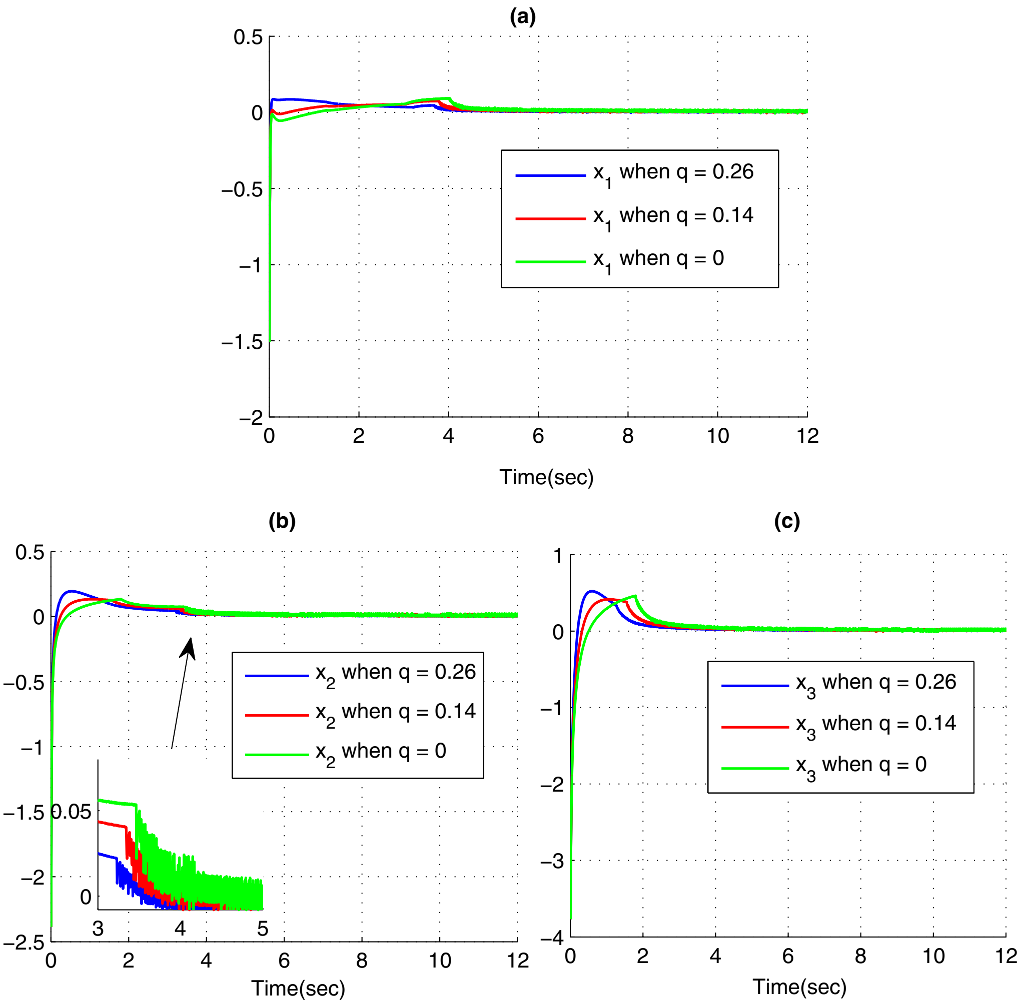

Fig. 9. Time responses of x_1, x_2, x_3 under the proposed FO exponential rate switching law $u_{sw} = -HD_t^q \mathrm{sgn}(s) - Ks$ with $q = 0.26, 0.14, 0$.

Now back to the fractional order case. According to [1,2], for the FO system $D_t^\beta \varsigma = \bar{A}\varsigma, \varsigma(0) = \varsigma_0, 0 < \beta < 1$, the system is asymptotically stable if and only if $|\arg(\lambda_j(\bar{A}))| > \beta\pi/2$. Clearly, due to $0 < \beta < 1$ and (19), it is straight forward to obtain

$$|\phi_j| = |\arg(\lambda_j(\bar{A}))| > \pi/2 \overset{0<\beta<1}{\Longrightarrow} |\arg(\lambda_j(\bar{A}))| > \beta\pi/2, \quad j = 1, 2, \ldots, n. \tag{20}$$

Hence, it is demonstrated that $D_t^\beta \varsigma = \bar{A}\varsigma, \varsigma(0) = \varsigma_0, 0 < \beta < 1$ is asymptotically stable if the IO system $D\varsigma = \bar{A}\varsigma, \varsigma(0) = \varsigma_0$ is asymptotically stable. This completes the proof. □

Remark 5.1. The matrix $\bar{A}$ is the same in both the IO system $Dx = \bar{A}x$ and the FO system $D_t^\beta \varsigma = \bar{A}\varsigma, 0 < \beta < 1$. Since that the stability condition of the IO system is $\mathrm{Re}(\lambda_j(\bar{A})) < 0, j = 1, 2, \ldots, n$, one concludes that the real part of all eigenvalues $\lambda_j(\bar{A})$ in the FO system are negative. Following the stability theorem of FO systems [1,2], the stability region SR_{FO} of the FO system with $0 < \beta < 1$ contains the stability region SR_{IO} of the IO system, i.e. $\mathrm{SR}_{FO} \supset \mathrm{SR}_{IO}$. Hence, one can conclude that $\lambda_i(\bar{A}) \in \mathrm{SR}_{FO}$ when $\lambda_i(\bar{A}) \in \mathrm{SR}_{IO}$. That is, due to $\mathrm{SR}_{FO} \supset \mathrm{SR}_{IO}$, all the eigenvalues of $D_t^\beta \varsigma = \bar{A}\varsigma, 0 < \beta < 1$ lie in SR_{FO} because they belong to SR_{IO}. Meanwhile, the stability condition $|\arg(\lambda_j(\bar{A}))| > \pi/2$ of the IO system can guarantee the stability condition $|\arg(\lambda_j(\bar{A}))| > \pi/2 > \beta\pi/2$ of the FO system with $0 < \beta < 1$. So, the FO system $D_t^\beta \varsigma = \bar{A}\varsigma, 0 < \beta < 1$ is asymptotically stable if the IO system $D\varsigma = \bar{A}\varsigma$ is asymptotically stable.

From (1) and (8), the sliding mode dynamics is obtained

$$\frac{d^\beta x(t)}{dt^\beta} = (-C_1^{-1}C_2\bar{K} - I + \delta(t))x(t), \quad y(t) = \Psi x(t). \tag{21}$$

Hence, the following theorem can ensure the robust stabilization of the system (21).

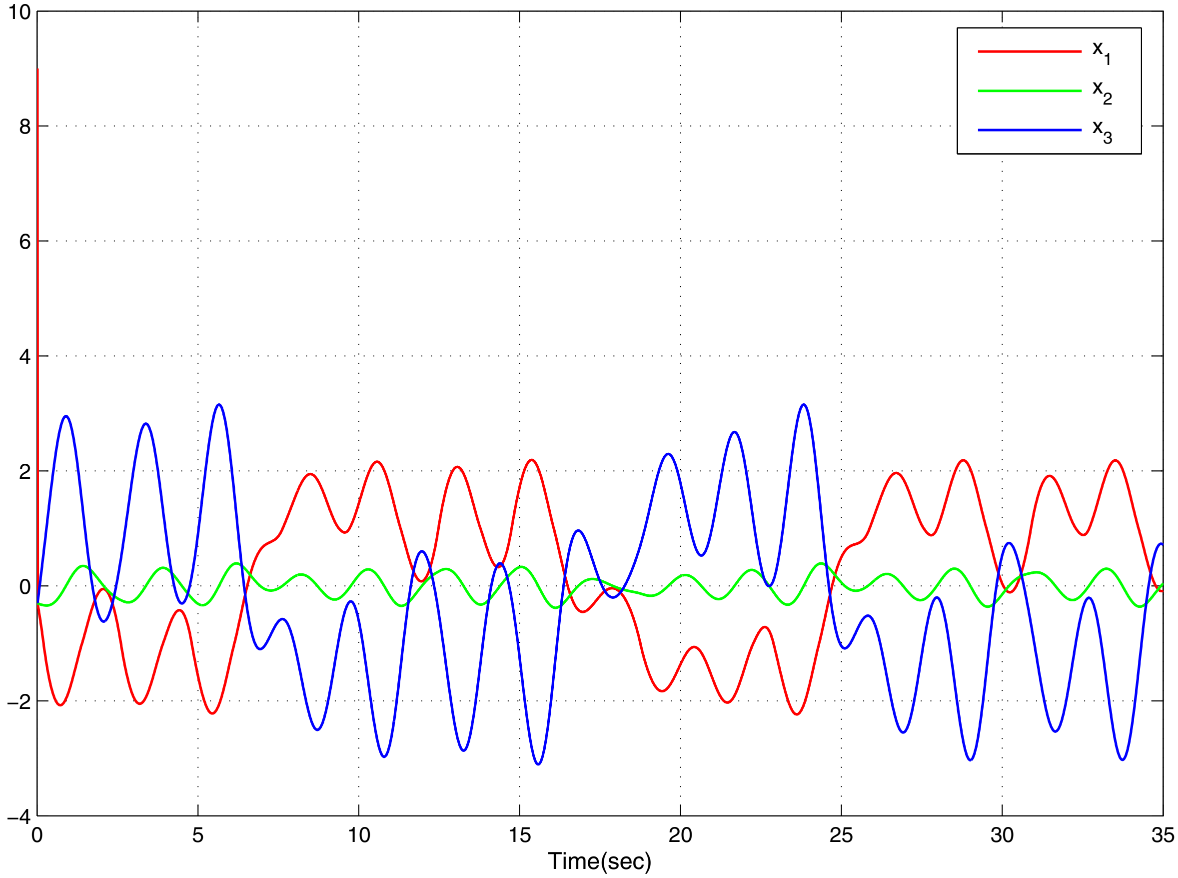

Fig. 10. Time responses of the FO Chua's circuit (31) without the controller and the uncertainty.

Theorem 5.1. *The sliding mode dynamics (21) is asymptotically stable if there exist a real symmetric positive matrix $\bar{P}$ and positive scalars ε_1, ε_2 satisfying the following LMI*

$$\begin{bmatrix} \Phi_{11} & 0 & N^T & 0 & \bar{P}W \\ * & -\varepsilon_1 I & 0 & \bar{P}W & 0 \\ * & * & -(\varepsilon_1 I)^{-1} & 0 & 0 \\ * & * & * & -\varepsilon_2 I & 0 \\ * & * & * & * & -\varepsilon_2 I \end{bmatrix} < 0, \tag{22}$$

where $\Phi_{11} = \bar{P}E + (\bar{P}E)^T + \varepsilon_2 N^T N$, $E = -C_1^{-1}C_2\bar{K} - I$.

Proof. For the FO sliding mode dynamic (21), the corresponding IO system can be derived $\frac{dx(t)}{dt} = (-C_1^{-1}C_2\bar{K} - I + \delta(t))x(t)$. Define $p(t) = G(t)q(t) = G(t)Nx(t)$. Then, the IO system can be rewritten by $\frac{dx(t)}{dt} = Ex(t) + Wp(t)$, where $E = -C_1^{-1}C_2\bar{K} - I$. Define $\xi(t) = [x^T(t) \quad p^T(t)]^T$. Construct the Lyapunov function $V(x(t)) = x^T\bar{P}x$, where $\bar{P} > 0$. The derivative of V can be obtained as

$$\dot{V} = \xi^T\left(\begin{bmatrix} \Phi & 0 \\ 0 & 0 \end{bmatrix} + \begin{bmatrix} \bar{P}\delta(t) + (\bar{P}\delta(t))^T & 0 \\ 0 & 0 \end{bmatrix}\right)\xi, \tag{23}$$

where $\Phi = \bar{P}E + (\bar{P}E)^T$. For the uncertainty, there exists $\varepsilon_2 > 0$ satisfying by Lemma 2.3,

$$\begin{bmatrix} \bar{P}(WG(t)N) + (WG(t)N)^T\bar{P} & 0 \\ 0 & 0 \end{bmatrix} \le \frac{1}{\varepsilon_2}\begin{bmatrix} 0 & \bar{P}W \\ \bar{P}W & 0 \end{bmatrix}\begin{bmatrix} 0 & W^T\bar{P} \\ W^T\bar{P} & 0 \end{bmatrix} + \varepsilon_2\begin{bmatrix} N^T N & 0 \\ 0 & 0 \end{bmatrix}. \tag{24}$$

On the other hand, the following inequality can be obtained $p^T(t)p(t) \le \xi^T(t)\bar{N}^T\bar{N}\xi(t)$, where $\bar{N} = [N \quad 0]$. Using the S-procedure [34], suppose there exists $\varepsilon_1 > 0$ satisfying

$$\begin{bmatrix} \bar{P}E + (\bar{P}E)^T & 0 \\ 0 & 0 \end{bmatrix} + \varepsilon_2\begin{bmatrix} N^T N & 0 \\ 0 & 0 \end{bmatrix} + \begin{bmatrix} 0 & 0 \\ 0 & -\varepsilon_1 I \end{bmatrix} + \bar{N}^T\varepsilon_1 I\bar{N} + \frac{1}{\varepsilon_2}\begin{bmatrix} 0 & \bar{P}W \\ \bar{P}W & 0 \end{bmatrix}\begin{bmatrix} 0 & W^T\bar{P} \\ W^T\bar{P} & 0 \end{bmatrix} < 0, \tag{25}$$

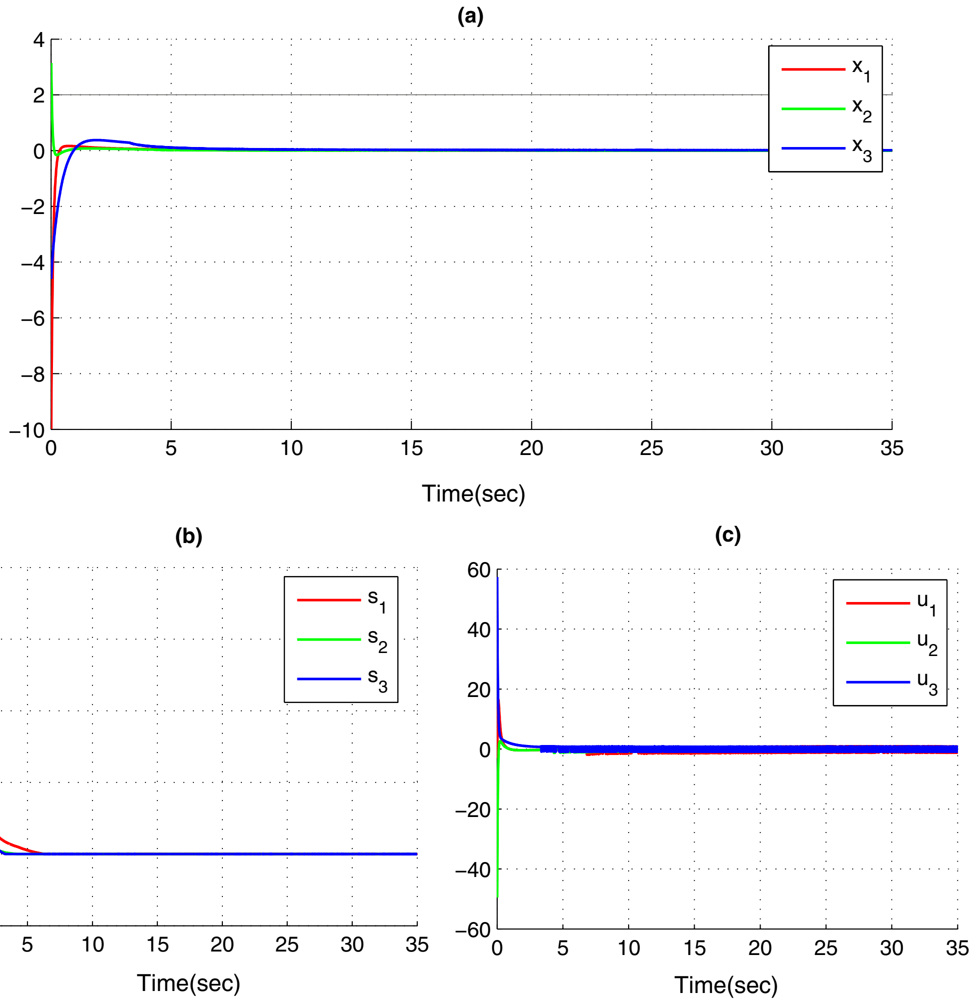

Fig. 11. Time responses of the Chua's circuit (31) under the controller (35); (b) the time response of the sliding surface (36); (c) the time response of the FO SMC (35).

then, one has $\dot{V} \leq 0$. By Lemma 2.4, (25) is satisfied if (22) holds. Hence, it guarantees the IO system asymptotic stability. From Proposition 5.1, LMI (22) holds, the sliding mode dynamics (21) is asymptotically stable. □

Remark 5.2. We remark that the FO exponential switching method with the FO sign function is not just limited for the FO nonlinear system (1). The FO exponential switching method with the FO sign function may be proposed for more general or more complex nonlinear systems. This will complicate the reachability analysis and stability analysis, including the calculation formula of reaching time since it appears to need to combine more generic or more intricate condition with the FO exponential rate switching law. We will further investigate the rule about how to select the fractional order $q_i \in [0, 1)$ of the FO exponential rate switching law in different systems, so as to obtain the better performance.

Remark 5.3. It should be mentioned that the linear matrix inequality (LMI) method has been widely developed to solve the problem of the stability of IO systems, including IO linear systems. Now, from Proposition 5.1, some interesting method based on LMI can be directly utilized to deal with the problem of the FO linear systems.

6. Numerical simulation

This section is utilized to show the advantages of the proposed control method.

Example 1. Consider the FO n-scroll attractor with uncertainty

$$D_t^{\beta} x = \left\{ \begin{bmatrix} -am_{2\iota} & a & 0 \\ 1 & -1 & 1 \\ 0 & -b & 0 \end{bmatrix} + \delta(t) \right\} x + \begin{bmatrix} 1 & 0 & 0 \\ 0 & 1 & 0 \\ 0 & 0 & 1 \end{bmatrix} \begin{bmatrix} f(x_1) \\ 0 \\ 0 \end{bmatrix} + \begin{bmatrix} 1 & 0 & 1 \\ 0 & 1 & 1 \\ 0 & 0 & 1 \end{bmatrix} u(t), \tag{26}$$

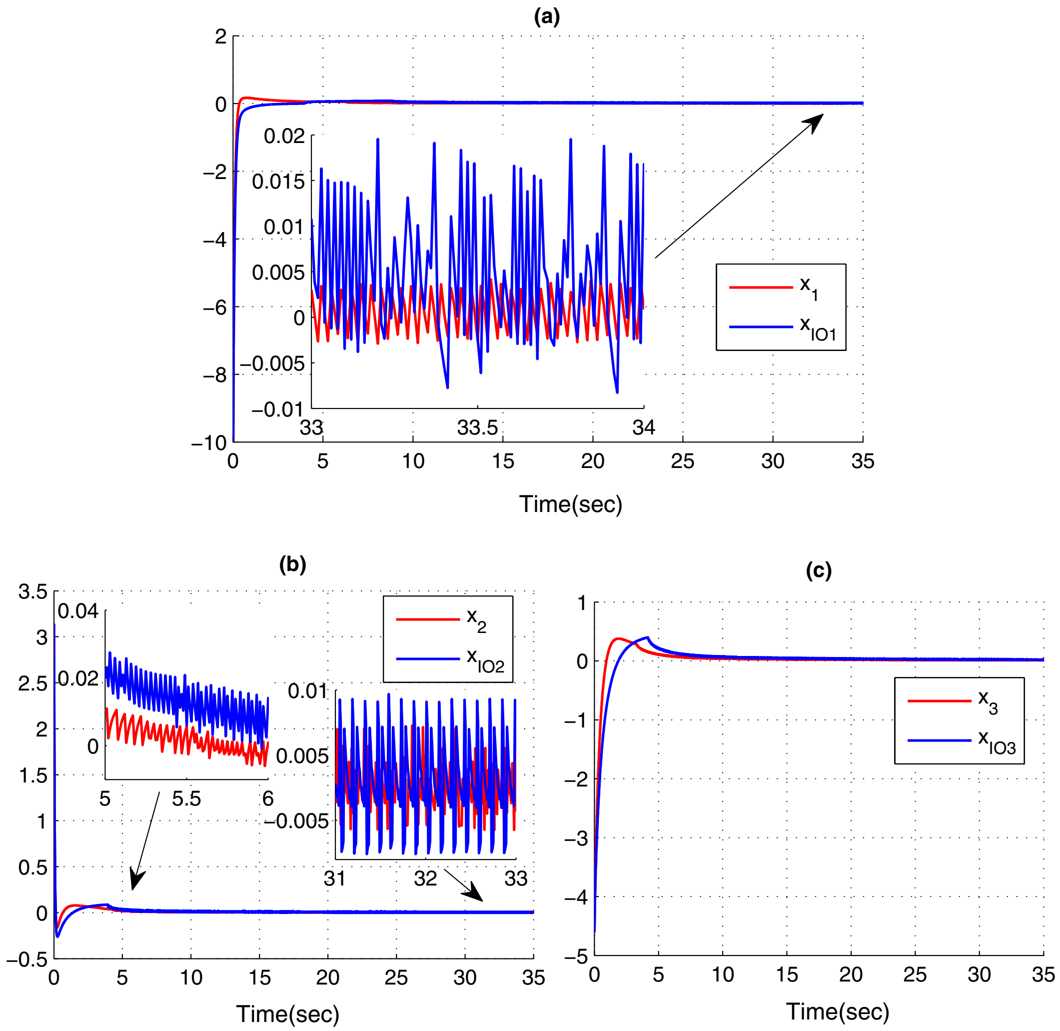

Fig. 12. Time responses of the states x_1, x_2, x_3 under the proposed controller (35), the states x_{IO1}, x_{IO2}, x_{IO3} under u_{IO}.

where $\beta = 0.87$, the uncertainty is

$$\delta(t) = \begin{bmatrix} 0.15\cos(0.2t) & 0 & 0 \\ 0 & 0.15\cos(0.2t) & 0 \\ 0 & 0 & 0.15\cos(0.2t) \end{bmatrix}.$$

And $f(x_1) = 0.5\sum_{i=1}^{2\iota-1}(m_i - m_{i+1})(|x_1 + c_i| - |x_1 - c_i|)$, $\iota = 3$. Here, the parameters are $c = [1, 2.15, 3.6, 6.2, 9]$, $m = [0.9/7, -3/7, 3.5/7, -2.7/7, 6/7, -2.4/7]$ and $a = 9$, $b = 14.28$. The uncertainty $\delta(t) = WG(t)N$ with

$$W = N = \begin{bmatrix} 1 & 0 & 0 \\ 0 & 1 & 0 \\ 0 & 0 & 1 \end{bmatrix}, \quad G(t) = \begin{bmatrix} \nu & 0 & 0 \\ 0 & \nu & 0 \\ 0 & 0 & \nu \end{bmatrix},$$

in which $\nu = 0.15\cos(0.2t)$. Let

$$C_1 = -\begin{bmatrix} 0.7813 & 0 & 0 \\ 0 & 0.7813 & 0 \\ 0 & 0 & 0.7813 \end{bmatrix}, \quad C_2 = \begin{bmatrix} 1 & 0 & 0 \\ 0 & 1 & 0 \\ 0 & 0 & 1 \end{bmatrix}, \quad K = \begin{bmatrix} 2.5 & 0 & 0 \\ 0 & 2.5 & 0 \\ 0 & 0 & 2.5 \end{bmatrix},$$

$$H = \begin{bmatrix} 0.315 & 0 & 0 \\ 0 & 0.315 & 0 \\ 0 & 0 & 0.315 \end{bmatrix}.$$

In the absence of the uncertainty, the time responses of the system (26) without the controller is depicted in Fig. 3.

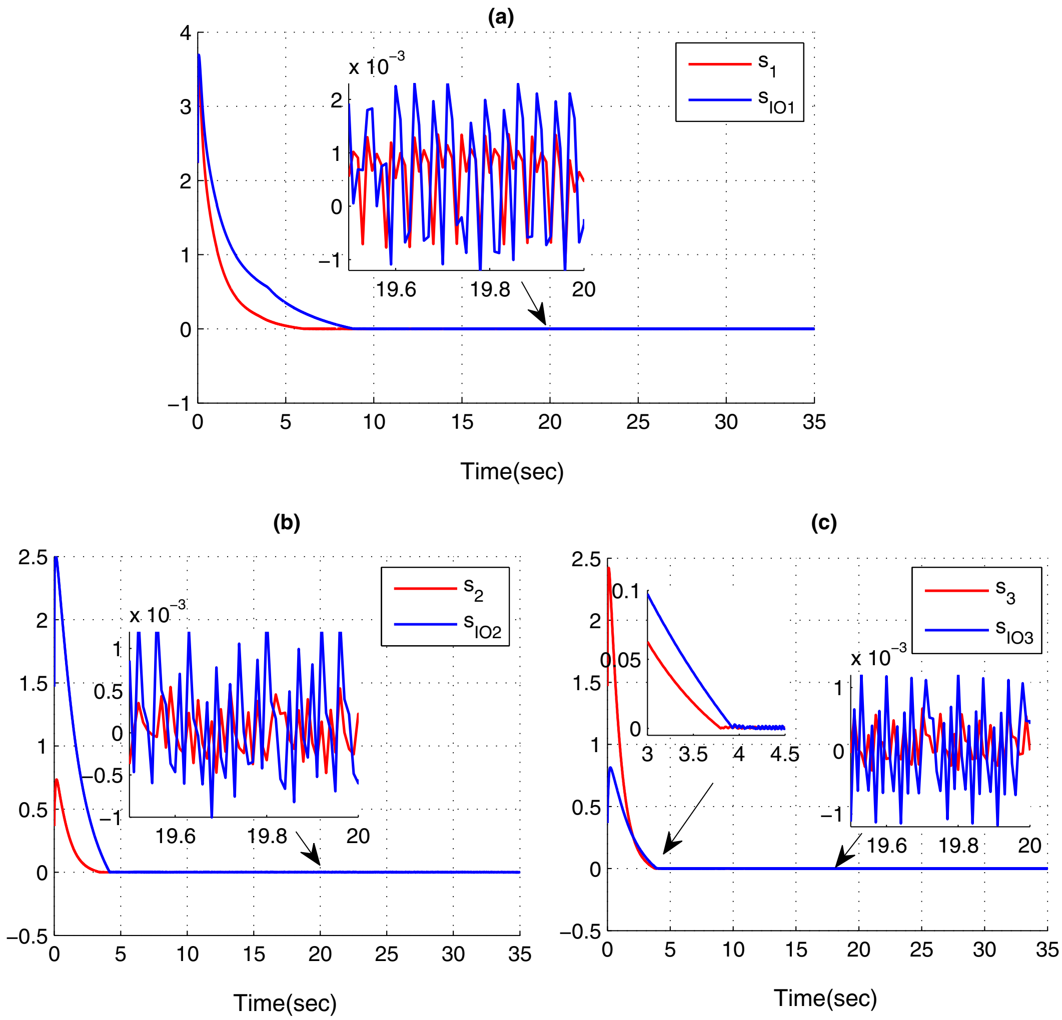

Fig. 13. Time responses of the sliding functions s_1, s_2, s_3 (36) under the proposed controller (35), s_{IO1}, s_{IO2}, s_{IO3} under u_{IO}.

By using Theorem 5.1, a feasible solution of the symmetric matrices and scalars is found using LMI Control Toolbox:

$$\bar{K} = -\begin{bmatrix} 3.5194 & 0 & 0 \\ 0 & 2.6478 & 0 \\ 0 & 0 & 1.5362 \end{bmatrix}, \quad \bar{P} = \begin{bmatrix} 0.7941 & 0.2892 & -0.2141 \\ 0.2892 & 0.8687 & 0.1646 \\ -0.2141 & 0.1646 & 0.9745 \end{bmatrix},$$
$$\varepsilon_1 = 0.1789, \varepsilon_2 = 0.2934. \tag{27}$$

From (8), we can obtain the following SMC:

$$u = \begin{bmatrix} -8.5903 & -23.2800 & 2.9662 \\ -1.0000 & -17.6690 & 1.9662 \\ 0 & 14.2800 & -2.9662 \end{bmatrix} x - \begin{bmatrix} 1 & 0 & -1 \\ 0 & 1 & -1 \\ 0 & 0 & 1 \end{bmatrix} f(x,t) + \begin{bmatrix} \varrho & 0 & -\varrho \\ 0 & \varrho & -\varrho \\ 0 & 0 & \varrho \end{bmatrix} \bar{u}, \tag{28}$$

in which $\varrho = 1.2799$, $\bar{u} = 0.7813||Nx||\mathrm{sgn}(s) - D_t^{1-\beta}s + HD_t^q\mathrm{sgn}(s) + Ks$ with $q = 0.12$. By Theorem 4.1, the system (26) under the controller (28) reaches the sliding surface

$$s = C_1 D_t^{-0.2}x + C_2 z, \quad \dot{z} = \bar{K}x - D_t^{0.2}z. \tag{29}$$

$[x_1(0), x_2(0), x_3(0)]^T = [-1.51, -2.39, -3.77]^T$ is the initial condition. The fractional integration operator is approximated via Carlson method in frequency range (0.01,100) rad/s by using MATLAB toolbox called Ninteger. Parts (a), (b) and (c) of Fig. 4 separately show the time responses of the states x_1, x_2, x_3, s in (29) and u in (28). It shows that u in (28) stabilizes the FO n-scroll attractor. Next, to demonstrate the better control performance of the proposed FO switching technique, some

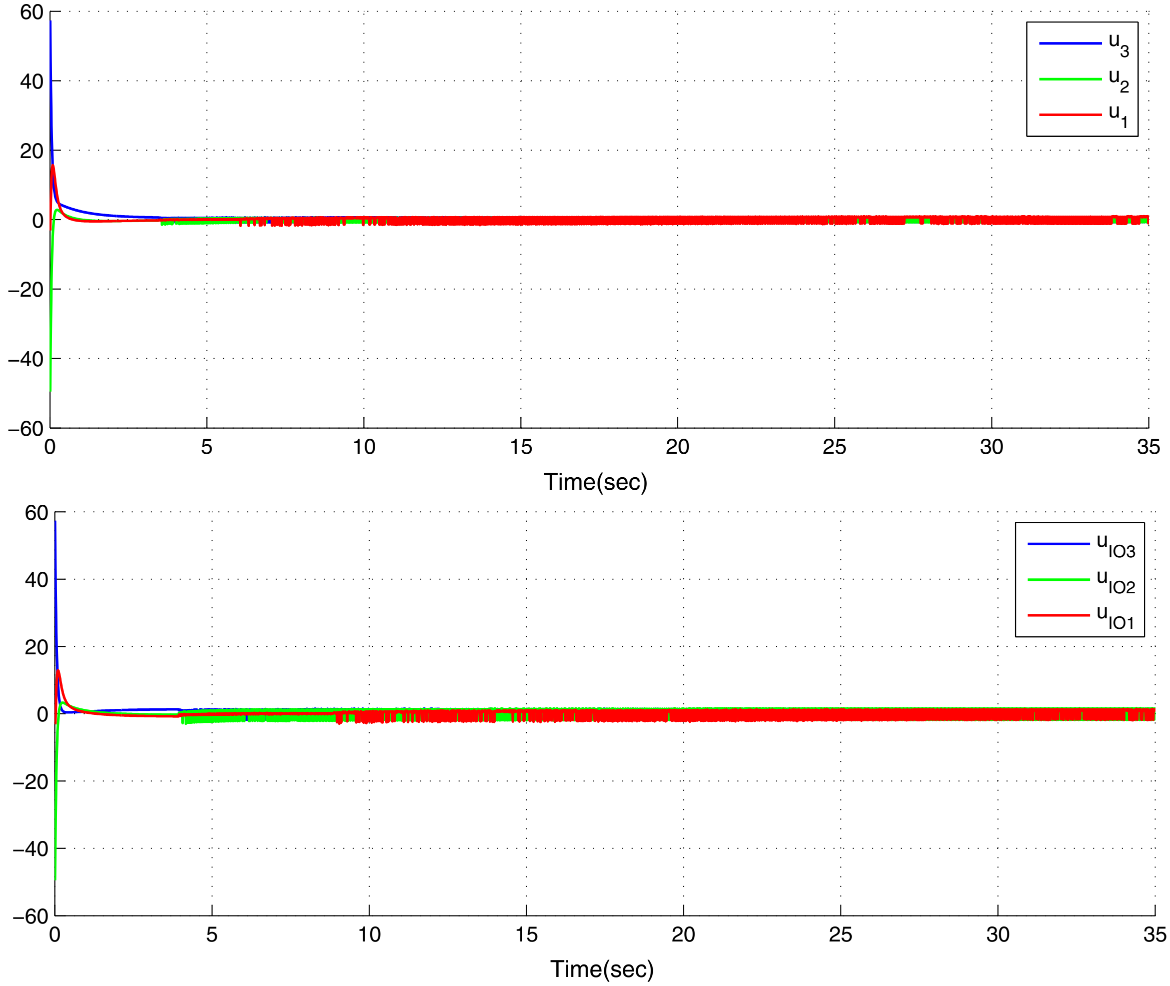

Fig. 14. Time responses of u and u_{IO}.

comparisons are provided. First, from the traditional IO switching law in [11,13], u_{IO-sw} is given by

$$u_{IO-sw} = -\begin{bmatrix} 0.685 & 0 & 0 \\ 0 & 0.875 & 0 \\ 0 & 0 & 1.415 \end{bmatrix} \operatorname{sgn}(s). \tag{30}$$

The sliding surface in the corresponding FO SMC u_{IO} with u_{IO-sw} is same as (29). To make this a fair comparison, the other parameters are remain the same in both of u and u_{IO}. Part (a) of Fig. 5 shows the comparison between x_1 under u and x_{IO1} under u_{IO}. Meanwhile, Parts (b) and (c) of Fig. 5 separately show the comparisons between x_2 under u and x_{IO2} under u_{IO}, x_3 under u and x_{IO3} under u_{IO}. The comparisons between the sliding surfaces s under u and s_{IO} under u_{IO} are presented in Fig. 6. Specifically, it can be seen that the reaching times of the sliding surfaces s_1, s_2 and s_3 under the proposed controller (28) are separately 3.9154, 3.3262 and 1.4732 in Fig. 6. Meanwhile, it can be found that the reaching times of the sliding surfaces s_1, s_2 and s_3 under the corresponding FO SMC u_{IO} with u_{IO-sw} are separately 4.7421, 3.5148 and 1.8357 in Fig. 6. It is clear that the reaching times under the FO exponential rate switching law are smaller than the reaching times under u_{IO-sw} in (30). Furthermore, the oscillating regions of s_1, s_2 and s_3 under the proposed controller (28) are approximately maintaining at $(-1.5\times10^{-3}, 2\times10^{-3})$, $(-1.2\times10^{-3}, 2\times10^{-3})$ and $(-2\times10^{-3}, 2\times10^{-3})$, respectively. In the meantime, the oscillating regions of s_1, s_2 and s_3 under the corresponding FO SMC u_{IO} with u_{IO-sw} are approximately maintained at $(-2\times10^{-3}, 3\times10^{-3})$, $(-2.1\times10^{-3}, 2.5\times10^{-3})$ and $(-2.5\times10^{-3}, 4\times10^{-3})$, respectively. It is obvious that the oscillations of s_1, s_2 and s_3 under the FO exponential rate switching law are decreased, when comparing with the oscillations of s_1, s_2 and s_3 under u_{IO-sw} in (30). The time responses of u, u_{IO} are drawn in Fig. 7. They show that the proposed FO SMC under the FO exponential rate switching law owns a faster and lower chattering performance.

Furthermore, in order to illustrate the potential benefits in adjusting the fractional-order q, the simulations are performed while the q is changed. The sliding functions $s = [s_1, s_2, s_3]^T$ under the proposed FO exponential rate switching law $u_{sw} =$

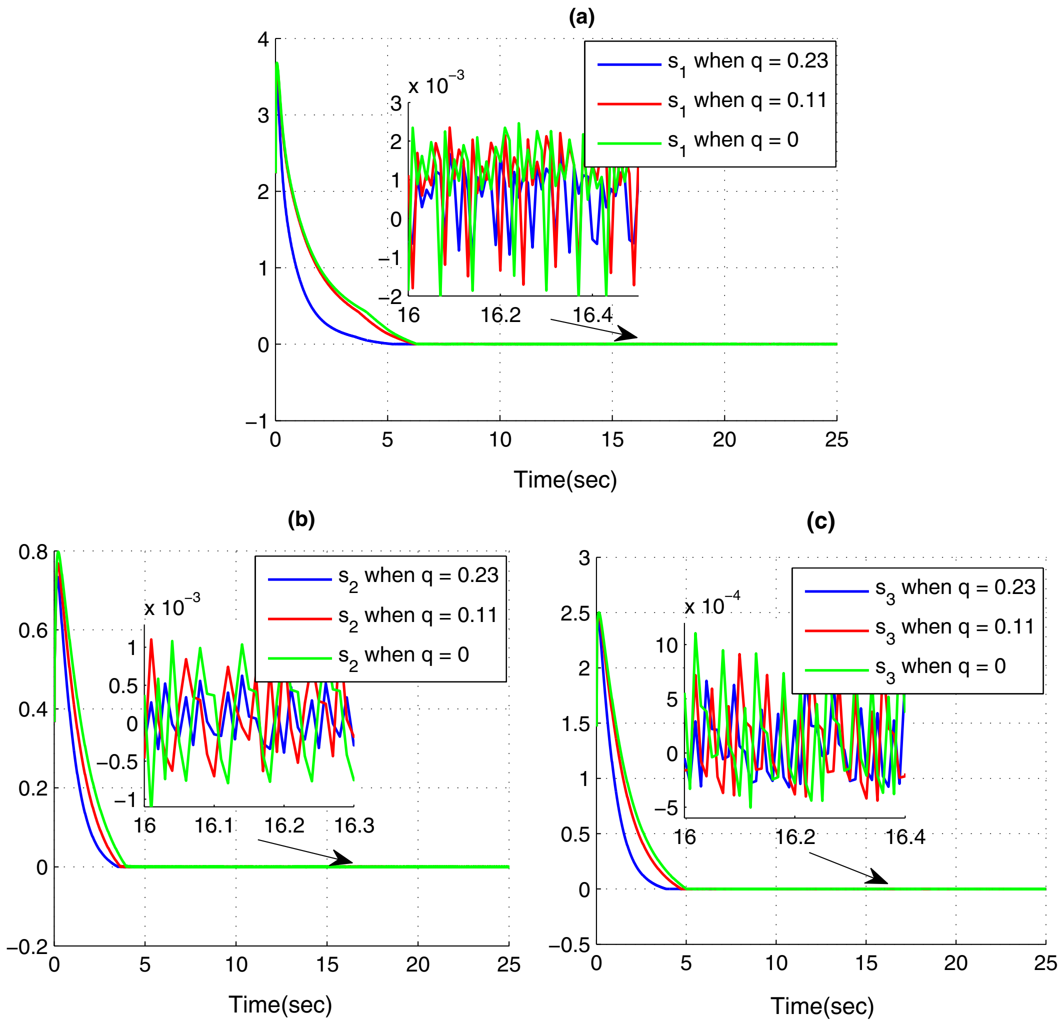

Fig. 15. Time responses of the sliding functions s_1, s_2, s_3 under the proposed FO exponential rate switching law $u_{sw} = -HD_t^q \mathrm{sgn}(s) - Ks$ with $q = 0.23, 0.11, 0$.

$-HD_t^q \mathrm{sgn}(s) - Ks$ with $q = 0.26, 0.14, 0$ are depicted in Fig. 8, when the other parameters of the SMC u are the same as (28). It can be seen that the reaching times of s_1, s_2, s_3 under u_{sw} with $q = 0.26, 0.14$ are smaller than the reaching times of s_1, s_2, s_3 under u_{sw} with $q = 0$. Meanwhile, the chattering phenomena of s_1, s_2, s_3 under u_{sw} with $q = 0.26, 0.14$ are smaller than the chattering of s_1, s_2, s_3 under u_{sw} with $q = 0$. Meanwhile, Fig. 9 shows the comparisons of $x = [x_1, x_2, x_3]^T$ under u_{sw} with $q = 0.26, 0.14, 0$. According to Figs. 8–9, the FO switching type control law u_{sw} can have better tracking performance including faster convergence speed and lower chattering performance by adjusting the fractional-order q.

Example 2. Consider the following FO Chua's circuit

$$D_t^\beta x = \begin{bmatrix} 18/7 + 0.15\cos(0.2t) & 9 & 0 \\ 1 & -1 + 0.15\cos(0.2t) & 1 \\ 0 & -14.78 & 0.15\cos(0.2t) \end{bmatrix} x + \begin{bmatrix} 1 & 0 & 0 \\ 0 & 1 & 0 \\ 0 & 0 & 1 \end{bmatrix} \begin{bmatrix} f(x_1) \\ 0 \\ 0 \end{bmatrix} + \begin{bmatrix} 1 & 0 & 1 \\ 0 & 1 & 1 \\ 0 & 0 & 1 \end{bmatrix} u(t), \tag{31}$$

with nonlinear characteristic $f(x_1) = 0.5(m_0 - m_1)(|x_1 + c| - |x_1 - c|)$ and parameters $c = 1, m_0 = -1/7, m_1 = 2/7, \beta = 0.98$. The uncertainty $\delta(t) = WU(t)N$ with

$$W = N = \begin{bmatrix} 1 & 0 & 0 \\ 0 & 1 & 0 \\ 0 & 0 & 1 \end{bmatrix}, U(t) = \begin{bmatrix} 0.15\sin(0.2t) & 0 & 0 \\ 0 & 0.1\sin(0.2t) & 0 \\ 0 & 0 & 0.1\sin(0.2t) \end{bmatrix}. \tag{32}$$

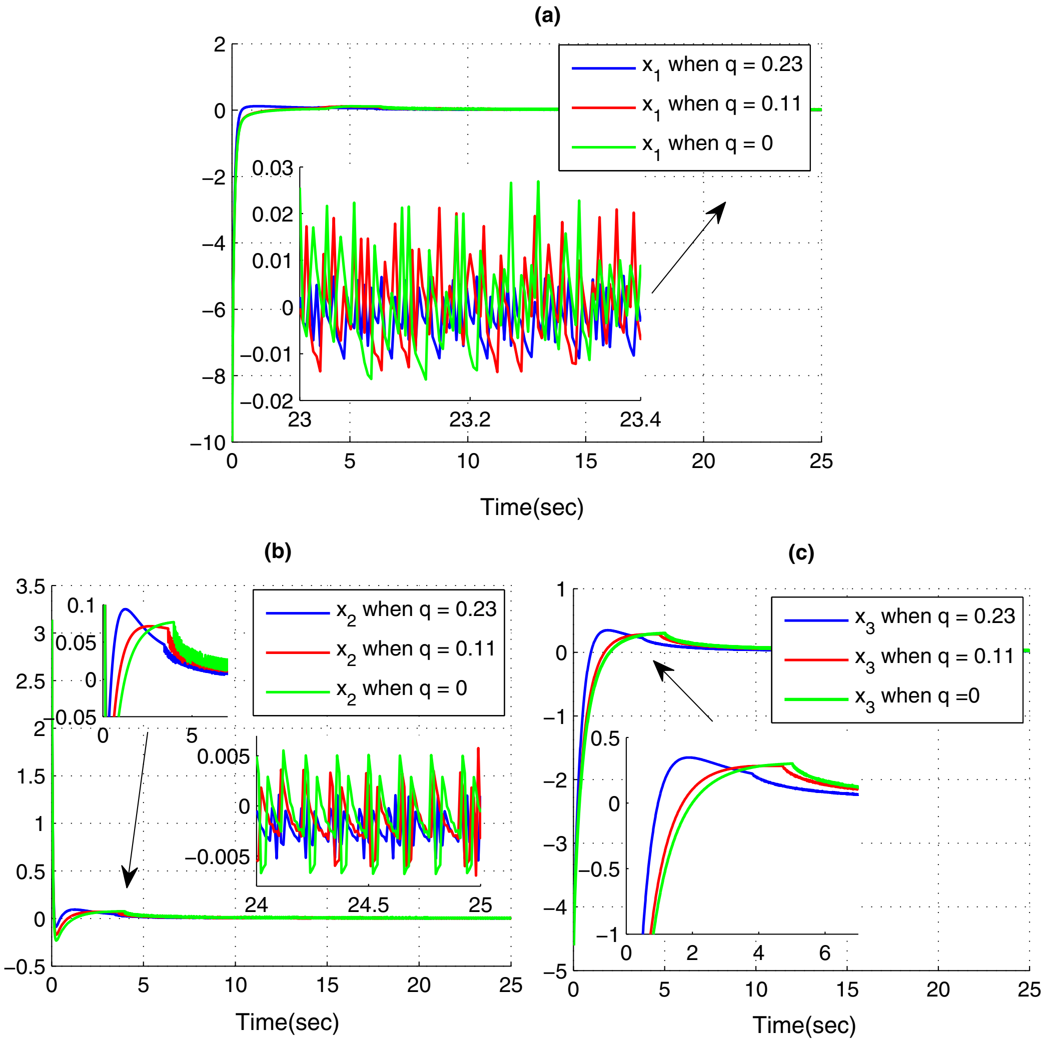

Fig. 16. Time responses of x_1, x_2, x_3 under the proposed FO exponential rate switching law $u_{sw} = -HD_t^q \mathrm{sgn}(s) - Ks$ with $q = 0.23, 0.11, 0$.

Let

$$C_1 = \begin{bmatrix} -0.5137 & 0 & 0 \\ 0 & -0.5137 & 0 \\ 0 & 0 & -0.5137 \end{bmatrix}, \quad C_2 = \begin{bmatrix} 1 & 0 & 0 \\ 0 & 1 & 0 \\ 0 & 0 & 1 \end{bmatrix},$$
$$K = \begin{bmatrix} 2.3 & 0 & 0 \\ 0 & 4.3 & 0 \\ 0 & 0 & 1.3 \end{bmatrix}, \quad H = \begin{bmatrix} 0.414 & 0 & 0 \\ 0 & 0.414 & 0 \\ 0 & 0 & 0.414 \end{bmatrix}. \tag{33}$$

In the absence of the uncertainty, the time responses of the system (31) without the controller are depicted in Fig. 10. By using Theorem 5.1 to the system (31), a feasible solution of the symmetric matrices and scalars is found using MATLAB LMI Control Toolbox:

$$\bar{K} = \begin{bmatrix} -2.2940 & 0 & 0 \\ 0 & -1.4758 & 0 \\ 0 & 0 & -0.4512 \end{bmatrix}, P = \begin{bmatrix} 0.5102 & -0.1775 & -0.0486 \\ -0.1775 & 0.0777 & 0.0375 \\ -0.0486 & 0.0375 & 1.2298 \end{bmatrix},$$
$$\varepsilon_1 = 8.5956, \varepsilon_2 = 5.0217. \tag{34}$$

By using (8), we can obtain the following SMC law:

$$u = \begin{bmatrix} -8.0371 & -23.7800 & 1.8783 \\ -1.0000 & -17.6529 & 0.8783 \\ 0 & 14.7800 & -1.8783 \end{bmatrix} x - \begin{bmatrix} 1 & 0 & -1 \\ 0 & 1 & -1 \\ 0 & 0 & 1 \end{bmatrix} f(x,t) + \begin{bmatrix} \varrho & 0 & -\varrho \\ 0 & \varrho & -\varrho \\ 0 & 0 & \varrho \end{bmatrix} \bar{u}, \tag{35}$$

in which $\varrho = 1.9467$ and $\bar{u} = 0.5137||Nx||\mathrm{sgn}(s) - D_t^{1-\beta} s + H^{RL}D_t^q \mathrm{sgn}(s) + Ks$ with $q = 0.1$.

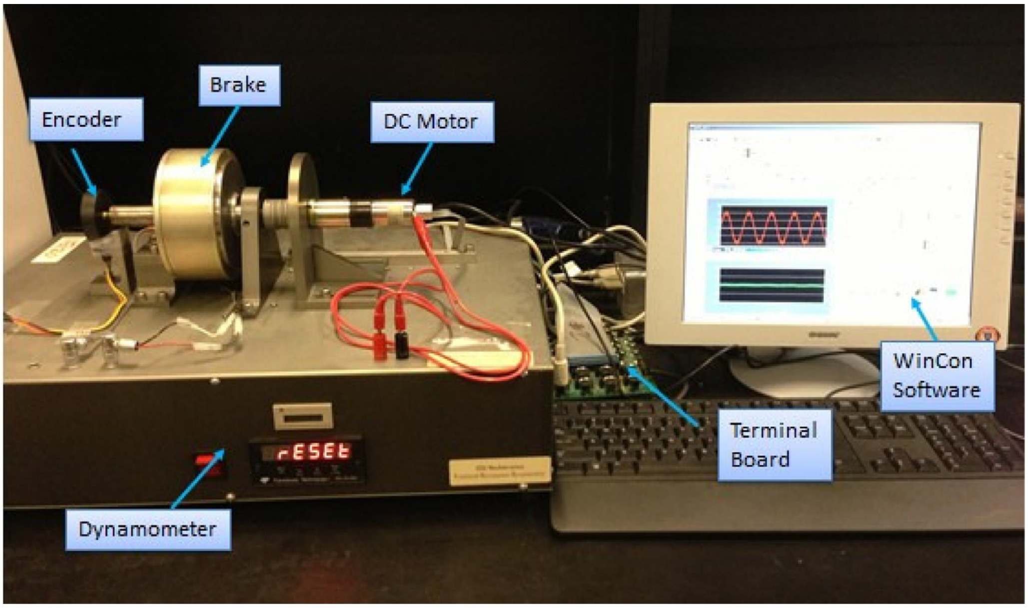

Fig. 17. The fractional horsepower dynamometer.

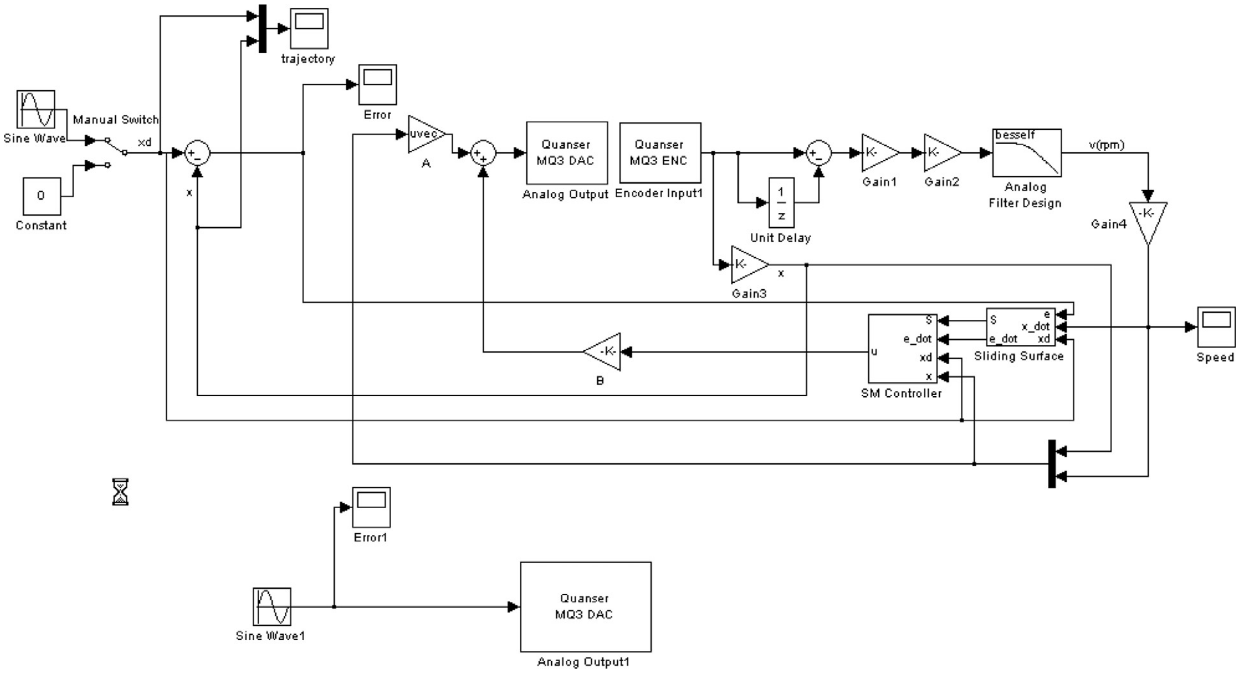

Fig. 18. Simulink/RTW model used in the SMC real time experiment using RTW Windows Target.

By Theorem 4.1, the system (31) under the controller (35), designed with the above parameters, converges to the sliding surface:

$$s = C_1 D_t^{-0.02} x + C_2 z, \quad \dot{z} = \bar{K} x - D_t^{0.02} z. \tag{36}$$

$[x_1(0), x_2(0), x_3(0)]^T = [-9.9848, 3.1414, -4.6052]^T$ is the initial condition. Parts (a),(b) and (c) of Fig. 11 separately show the time responses of the states x_1, x_2, x_3, s in (36) and u in (35). It shows that u in (35) stabilizes the FO Chua's circuit. Next, in order to show the better control performance of the proposed FO switching technique, some comparisons are provided.

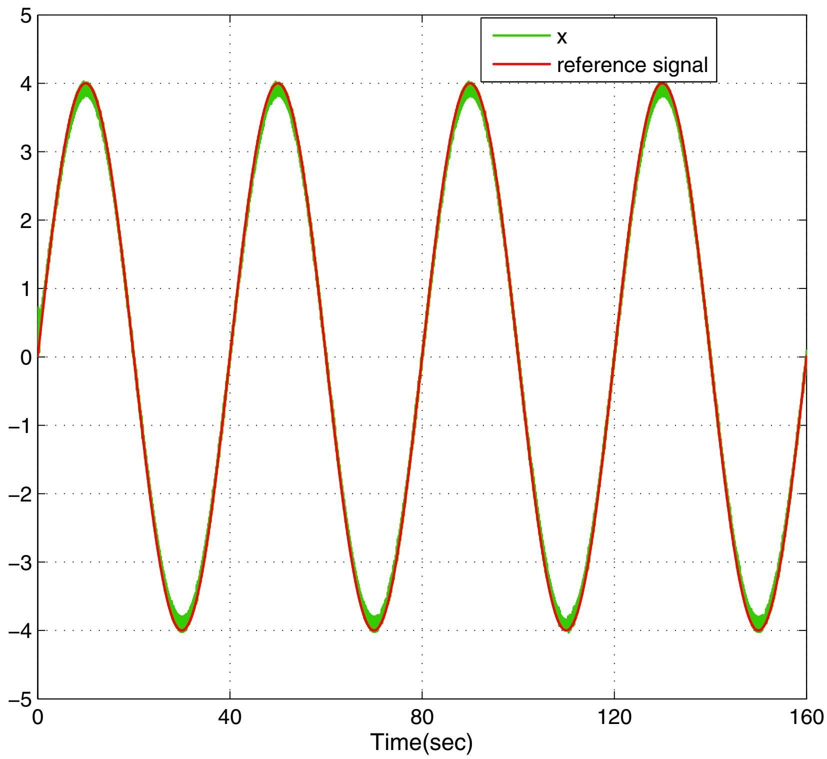

Fig. 19. Position tracking under the FO exponential rate switching law with $q = 0.1$.

First, from the traditional IO switching law in [11,13], u_{IO-sw} is given by

$$u_{IO-sw} = -\begin{bmatrix} 0.914 & 0 & 0 \\ 0 & 1.015 & 0 \\ 0 & 0 & 0.914 \end{bmatrix} \mathrm{sgn}(s). \tag{37}$$

The sliding surface in the corresponding FO SMC u_{IO} with u_{IO-sw} is same as (36). Moreover, the other parameters are same in both of u and u_{IO}, so as to do the fair comparison. Part (a) of Fig. 12 shows the comparison between x_1 under u and x_{IO1} under u_{IO}. Meanwhile, Parts (b) and (c) of Fig. 12 separately show the comparisons between x_2 under u and x_{IO2} under u_{IO}, x_3 under u and x_{IO3} under u_{IO}. The comparisons between the sliding surfaces s under u and s_{IO} under u_{IO} are presented in Fig. 13. Specifically, it can be seen that the reaching times of the sliding surfaces s_1, s_2 and s_3 under the proposed controller (35) are separately 5.6427, 3.785 and 3.7514 in Fig. 6. Meanwhile, it can be found that the reaching times of the sliding surfaces s_1, s_2 and s_3 under the corresponding FO SMC u_{IO} with u_{IO-sw} are separately 8.9735, 4.2109 and 3.9023 in Fig. 6. It is clear that the reaching times under the FO exponential rate switching law are smaller than the reaching times under u_{IO-sw} in (37). Furthermore, the oscillating regions of s_1, s_2 and s_3 under the proposed controller (35) are approximately maintained at $(-1\times10^{-3}, 1.4\times10^{-3})$, $(-0.5\times10^{-3}, 0.5\times10^{-3})$ and $(-0.3\times10^{-3}, 0.5\times10^{-3})$, respectively. In the meantime, the oscillating regions of s_1, s_2 and s_3 under the corresponding FO SMC u_{IO} with u_{IO-sw} are approximately maintaining at $(-1.5\times10^{-3}, 2.5\times10^{-3})$, $(-1.1\times10^{-3}, 1.6\times10^{-3})$ and $(-1.1\times10^{-3}, 1.3\times10^{-3})$, respectively. It is obvious that the oscillations of s_1, s_2 and s_3 under the FO exponential rate switching law are reduced, when comparing with the oscillations of s_1, s_2 and s_3 under u_{IO-sw} in (30). The time responses of u and u_{IO} are drawn in Fig. 14. They show that the proposed FO SMC under the FO exponential rate switching law owns a faster and lower chattering performance.

Moreover, the simulations are performed while q is changed, in order to show potential benefits in adjusting q. The sliding functions $s = [s_1, s_2, s_3]^T$ under the proposed FO exponential rate switching law $u_{sw} = -HD_t^q \mathrm{sgn}(s) - Ks$ with $q = 0.23, 0.11, 0$ are depicted in Fig. 15, when the other parameters of the SMC u are the same as (35). It can be seen that the reaching times of s_1, s_2, s_3 under u_{sw} with $q = 0.23, 0.11$ are smaller than the reaching times of s_1, s_2, s_3 under u_{sw} with $q = 0$. Meanwhile, the chattering phenomena of s_1, s_2, s_3 under u_{sw} with $q = 0.23, 0.11$ are smaller than the chattering of s_1, s_2, s_3 under u_{sw} with $q = 0$. Meanwhile, Fig. 16 shows the comparisons of $x = [x_1, x_2, x_3]^T$ under u_{sw} with $q = 0.23, 0.11, 0$. According to Figs. 15–16, the FO switching type control law u_{sw} can have better tracking performance including faster convergence speed and lower chattering performance by adjusting the fractional-order q.

Remark 6.1. Examples 1–2 verify the effectiveness and advantages of the proposed control method with the FO exponential switching technique for the FO nonlinear system (1). In addition, as mentioned in Remark 5.2, the proposed FO exponential

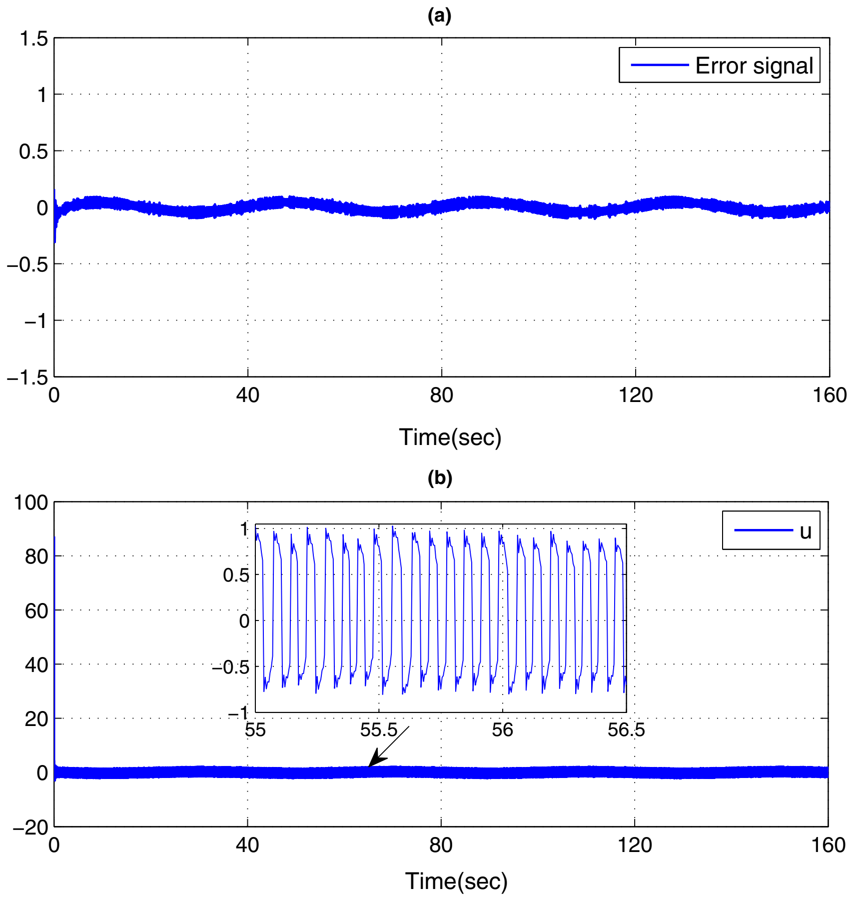

Fig. 20. The corresponding error signal and the controller u under the FO exponential rate switching law with $q = 0.1$.

switching technique is not just limited for the FO nonlinear system (1). Next, the proposed FO exponential rate switching law will be applied for the real nonlinear system, to show the practicality of the FO exponential switching technique. That is, the proposed FO exponential rate switching law is implemented into a fractional horsepower dynamometer position servo system shown in Fig. 17. The dynamometer mainly involves a DC motor, a hysteresis brake, an optical encoder and a tachometer. It is also linked to a Quanser Q4 terminal board for the system control through the Matlab/Simulink Real-Time Workshop (RTW) software. The servo control system can be modeled by $\dot{x} = v, \dot{v} = Bu + \rho(t, v)$ where x, v and $\rho(t, v)$ denote the position state, the velocity and the disturbance. u represents the control input with the gain coefficient B. In [6,35,36], the DC motor of dynamometer is identified by $G_m(s) = \frac{1.52}{1.01s+1}$.

To demonstrate the practicality of the FO exponential switching technique, a position tracking control will be performed through SMC with the FO exponential rate switching law. In the following, we will utilize the brake to carry out the position tracking experiment. Let the reference signal $r(t) = 4\sin((2\pi/40)t)$. The FO exponential rate switching law and sliding surface are chosen by $u_{sw} = -0.85D^{0.1}\mathrm{sgn}(s) - s$ and $s = e + \dot{e}$ where $e = r - x$. Fig. 18 displays the Simulink model implemented in the experiment. Figs. 19 and 20 show the tracking results. As depicted in Fig. 18, the disturbance $0.1\sin(t)$ is append to the Magtrol Hysteresis Brake, to verify the robust property of the FO exponential rate switching law. The experimental result shows the practicality of the proposed FO exponential switching technique.

7. Conclusion

This paper has introduced the FO SMC with the FO exponential rate switching law and the FO PI sliding surface for uncertain FO nonlinear systems. The FO sign function $D_t^q\mathrm{sgn}(s), 0 \le q < 1$ has been developed to construct the FO exponential rate switching law. The FO exponential rate switching law has been proven to guarantee the reaching phase in finite time. The reaching time t_{reach} has been analytically derived, for the first time. The reachability analysis has been illustrated and visualized to disclose how the control performance is improved. The stability condition of the FO sliding mode dynamics has been derived based on the stable region analysis and the Lyapunov stability method. Finally, simulation results have been given to show the advantages of the designed control scheme. Future work will focus on built a tuning mechanism in its full generality for the controller parameters including q_i. The rule about how to select $q_i \in [0, 1)$ of the FO exponential rate switching law in different systems will be investigated, in order to obtain the better performance.

References

[1] D. Matignon, Stability results for fractional differential equations with applications to control processing, in: Proceedings of the IMACS-SMC, Lille, France, 1996, pp. 963–968.
[2] J. Sabatier, M. Moze, C. Farge, LMI stability conditions for fractional order systems, Comput. Math. Appl. 59 (2010) 1594–1609.
[3] Y. Li, Y.Q. Chen, I. Podlubny, Mittag-leffler stability of fractional-order nonlinear dynamic systems, Automatica 45 (2009) 1965–1969.
[4] D. Sierociuk, W. Malesza, M. Macias, Derivation, interpretation, and analog modelling of fractional variable order derivative definition, Appl. Math. Model. 39 (2015) 3876–3888.
[5] I. Podlubny, Fractional-order systems and $PI^{\lambda}d^{\mu}$-controllers, IEEE Trans. Automat. Contr. 44 (1999) 208–214.
[6] C. Yin, Y.Q. Chen, S.M. Zhong, Fractional-order sliding mode based extremum seeking control of a class of nonlinear systems, Automatica 50 (2014) 3173–3181.
[7] C. Yin, B. Stark, Y.Q. Chen, S.M. Zhong, E. Lau, Fractional-order adaptive minimum energy cognitive lighting control strategy for the hybrid lighting system, Energy Build. 15 (2015) 176–184.
[8] H. Malek, S. Dadras, Y.Q. Chen, Performance analysis of fractional order extremum seeking control, ISA Trans. 61 (2016) 281–287.
[9] R. Behinfaraz, M. Badamchizadeh, A.R. Ghiasi, An adaptive method to parameter identification and synchronization of fractional-order chaotic systems with parameter uncertainty, Appl. Math. Model. 40 (2016) 4468–4479.
[10] V.I. Utkin, Sliding Modes in Control and Optimization, New York: Springer-Verlag, 1992.
[11] C. Edwards, E. Fossas, L. Fridman, Advances in Variable Structure and Sliding Mode Control Lecture Notes in Control and Information Science, New York: Springer-Verlag, 2006.
[12] A. Pisano, M.R. Rapaic, Z.D. Jelicic, E. Usai, Sliding mode control approaches to the robust regulation of linear multivariable fractional-order dynamics, Int. J. Robust Nonlinear Control 20 (18) (2010) 2045–2056.
[13] J.K. Liu, X.H. Wang, Advanced Sliding Mode Control for Mechanical Systems: Design, Analysis and MATLAB Simulation, Berlin: Springer, Beijing: Tsinghua University Press, 2012.
[14] Y. Feng, F. Han, X. Yu, Chattering free full-order sliding-mode control, Automatica 50 (2014) 1310–1314.
[15] J. Hua, L. An, Y. Li, Bionic fuzzy sliding mode control and robustness analysis, Appl. Math. Model. 39 (2015) 4482–4493.
[16] J. Juang, S. Yu, Disturbance encountered landing system design based on sliding mode control with evolutionary computation and cerebellar model articulation controller, Appl. Math. Model. 39 (2015) 5862–5881.
[17] A. Si-Ammour, S. Djennoune, M. Bettayeb, A sliding mode control for linear fractional systems with input and state delays, Commun. Nonlinear Sci. Numer. 14 (2009) 2310–2318.
[18] M.S. Tavazoei, M. Haeri, Synchronization of chaotic fractional-order systems via active sliding mode controller, Phys. A 387 (2008) 57–70.
[19] C. Yin, S.M. Zhong, W. Chen, Design of sliding mode controller for a class of fractional-order chaotic systems, Commun. Nonlinear Sci. Numer. 17 (2012) 356–366.
[20] N. Yang, C. Liu, A novel fractional-order hyperchaotic system stabilization via fractional sliding-mode control, Nonlinear Dyn. 74 (2013) 721–732.
[21] C. Yin, S. Dadras, S.M. Zhong, Y.Q. Chen, Control of a novel class of fractional-order chaotic systems via adaptive sliding mode control approach, Appl. Math. Model. 37 (2013) 2469–2483.
[22] G. Zhong, H. Deng, J. Li, Chattering-free variable structure controller design via fractional calculus approach and its application, Nonlinear Dyn. 81 (2015) 679–694.
[23] B. Zhang, Y. Pi, Y. Luo, Fractional order sliding-mode control based on parameters auto-tuning for velocity control of permanent magnet synchronous motor, ISA Trans. 51 (2012) 649–656.
[24] Y. Tang, X. Zhang, D. Zhang, G. Zhao, X. Guan, Fractional order sliding mode controller design for antilock braking systems, Neurocomput. 111 (2013) 122–130.
[25] M.P. Aghababa, A fractional sliding mode for finite-time control scheme with application to stabilization of electrostatic and electromechanical transducers, Appl. Math. Model. 39 (2015) 6103–6113.
[26] S. Ebrahimkhani, Robust fractional order sliding mode control of doubly-fed induction generator (DFIG)-based wind turbines, ISA Trans. 63 (2016) 343–354.
[27] S. Dadras, H.R. Momeni, Passivity-based fractional-order integral sliding-mode control design for uncertain fractional-order nonlinear systems, Mechatronics 23 (7) (2013) 880–887.
[28] S. Chakrabarty, B. Bandyopadhyay, A generalized reaching law for discrete time sliding mode control, Automatica 52 (2015) 83–86.
[29] A. Bartoszewicz, P. Lesniewski, New switching and non-switching type reaching laws for SMC of discrete time systems, IEEE Trans. Control Syst. Technol. 24 (2) (2016) 670–677.
[30] C. Yin, Y.Q. Chen, S.M. Zhong, Fractional-order power rate type reaching law for sliding mode control of uncertain nonlinear system, in: Proceedings of 19th IFAC, Cape Town, South Africa, 2014, pp. 5369–5374.
[31] C. Yin, Y. Cheng, Y.Q. Chen, B. Stark, S.M. Zhong, Adaptive fractional-order switching-type control method design for 3d fractional-order nonlinear systems, Nonlinear Dyn. 82 (2015) 39–52.
[32] D. Matignon, Stability properties for generalized fractional differential systems, ESAIM: Proc. 5 (1998) 145–158.
[33] S. Boyd, L.E. Ghaoui, E. Feron, V. Balakrishnan, Linear Matrix Inequalities in System and Control Theory, SIAM, Philadelphia, PA, 1994.
[34] H.K. Khalil, Nonlinear Systems, 3rd ed., Prentice Hall, 2002.
[35] H. Malek, S. Dadras, Y.Q. Chen, A fractional order maximum power point tracker: stability analysis and experiments, in: Proceedings of 51th IEEE Conference on Decision and Control, 2012, pp. 6861–6866.
[36] H. Malek, S. Dadras, Y.Q. Chen, Performance analysis of fractional order extremum seeking control, ISA Trans. 63 (2016) 281–287.